European Photochemistry Association

NEWSLETTER

No. 86, June 2014

General information about the European

Photochemistry Association

is available at:

www.photochemistry.eu

Newsletter Editor: Prof. Maurizio D'Auria

Dipartimento di Scienze
Università della Basilicata
85100 Potenza, ITALY

ISSN 1011-4246

Printed in the United Kingdom by Media Services, Loughborough University, Leicestershire LE11 3TU

CONTENTS

EPA EXECUTIVE COMMITTEE

President

Prof. Dr. Werner NAU
School of Engineering and Science of Chemistry, Jacobs University
Campus Ring 1
D-28759 BREMEN
Germany
Email: w.nau@jacobs-university.de

Industry-Liaison

Dr. John Gilchrist
Gilden Photonics Ltd.
Unit 13 Telford Court, 9 South Avenue
Clydebank Business Park
Glasgow, G81 2NR, UK
Tel: +44(0)141.952.9475
Email:
john.gilchrist@gildenphotonics.com

Treasurer

Dr. Alexandre Fürstenberg
Department of Human Protein Sciences
University of Geneva
1211 Genève 4, Switzerland
Tel: +41 22 379 54 73
Fax: +41 22 379 55 02
Email: Alexandre.Fuerstenberg@unige.ch

Public Relations

Prof. Dr. Olga Fedorova
A.N.Nesmeyanov Institute of
Organoelement Compounds
Russian Academy of Sciences
28 Vavilova St., Moscow
RUSSIA 119991
Tel: +7 499 135 8098
Email: fedorova@ineos.ac.ru

Past President and PPS matters:

Prof. Dr. Eric Vauthey
Department of Physical Chemistry
University of Geneva
30 quai Ernest-Ansermet,
CH-1211 Geneve 4
Switzerland
Tel +41(0)22 379 6537
Email: eric.vauthey@unige.ch

Newsletter Editor:

Prof. Maurizio D'Auria
Dipartimento di Scienze
Università della Basilicata
Viale dell'Ateneo Lucano 10
85100 Potenza
Italy
Emal: maurizio.dauria@unibas.it

Associate Editor:

Prof. Julia Pérez-Prieto
Molecular Science Institute (ICMOL)
Valencia University
C/ Catedrático José Beltrán, 2
46980-Paterna, Valencia, Spain
Tel: +34-96-3543050
Email: julia.perez@uv.es

Website manager:

Dr. David Worrall
Photochemistry Research Group
Department of Chemistry
Loughborough University
Leicestershire LE11 3TU, UK
Tel: +44(0)1509 222567
Email: d.r.worrall@lboro.ac.uk

New Information Technologies

Prof. Dr. Roberto Improta
Institute for Biostructures and
Bioimaging
Naples
Email: robimp@unina.it

EDITORIAL

President's Letter

Dear EPA members

While our society journal *Photochemical & Photobiological Sciences* (PPS) is flourishing, we have an important upcoming change to announce, that of the Editor-in-Chief. It is my particular pleasure to let you know that the Ownership Board of PPS, following the nomination by the Executive Committee (EC) of EPA, was able to appoint for this important position Dario Bassani, Bordeaux, as successor of Frans de Schryver, Leuven. Frans de Schryver has served PPS, and therefore EPA, since 2006, and he has launched the journal from its start-up phase (under the founding Editor-in-Chief Frank Wilkinson, Loughborough) into a prominent position of the science landscape, and very well placed in comparison to its direct competitor journals specializing on photochemistry content. Accordingly, the impact factor stands at an excellent value of around 3 during the past years. I was hoping to include the latest value into this letter, but publication of the *Journal Citation Reports* this year appears to deviate from the traditional mid-June date.

I would like to take the opportunity, on behalf of the EC and EPA, to cordially thank Frans de Schryver for the long-term work he has done for PPS. At the same time, I encourage all members to continue to support the journal and Dario Bassani as our new Editor-in-Chief of PPS.

I am happy to report that the membership numbers of EPA have remained at a constant, high level during the past years, and even if some European countries are still lagging behind expectation in regard to the number of members in EPA, we have been able to keep the membership fees at a low level, making EPA attractive to both, advanced researchers and students. In fact, starting this year, we have introduced discounted long-term memberships (3-years and 5-years), which are receiving positive feedback, greatly simplifying the administrative burden on both, the members' and the treasurer's side. Of course, electronic access to PPS remains free for all EPA members also in the foreseeable future.

This year, EPA has administered or pre-selected three awards in the area of photochemistry, the *EPA-PPS Prize* for the most highly cited paper published in PPS during the foregoing two calendar years, the *EPA Prize for Best PhD Thesis in Photochemistry* published during the forgoing two calendar years, and the *Porter Medal*, in cooperation with our Inter-American and Asian/Oceanian photochemistry association counterparts, I-APS and APA. All three prizes are being awarded during the XXVth IUPAC Symposium on Photochemistry held in Bordeaux in July 2014, chaired also by Dario Bassani.

The composition of the EC will undergo in 2014 its biannual statutory changes during the IUPAC Symposium, where our General Council is being held, and all members have received a separate email on this matter. Important to note, our association remains to draw protagonists who are willing to take over important tasks on behalf of our association in the EC, ranging from the two editors of our *EPA Newsletter*, the treasurer, the website manager, and the representatives for new information technologies, PPS matters, public relations, as well as industry liaison. In the years to come, I look forward to support the work of the EC and EPA as Past-President.

Prof. Werner Nau
Jacobs University, Bremen

PUBLICATIONS

Some questions on Horizon 2020

We asked some questions to Mrs Pascale Dupont of the Key Enabling Technologies ofl Research & Innovation Direction of the European Commision.
The views expressed in this interview are the sole responsibility of the author and do not necessarily
reflect the views of the European Commission.

1. **How the process of defining the priorities of the scientific agenda (e.g. the themes of Horizon 2020) of the EU works?**

   First, Horizon 2020 does not have "themes" like the ones in FP7, as it aims for a more integrated, challenge-based approach. The priorities in each Work Programme originate from many different inputs, including industrial roadmaps and policy needs in particular. The Commission develops rolling multi-annual strategies and Work Programmes, which are adopted by the Commission after a consultation process with the Member States.

2. **What is the possible role of an European Scientific Association as EPA in this process?**

   A wide range of stakeholders are consulted in the course of developing each Work Programme. In addition to industry which participates in European Technology Platforms and similar bodies, scientific associations also play a prominent role in the process: they are often represented in Advisory Groups, which help the Commission identify and implement priorities, as well as in relevant European technology Platforms. The memberships of all these groupings are in the

public domain. European Technology Platforms and Public-Private Partnership Boards are always open to interested newcomers.

3. **Is it provided a space for discussing the issues related to scientific policy of EU with organizations as EPA, beyond the internet tools (IPM) in the** http://ec.europa.eu/research/ **site, that seems oriented towards individuals?**

   The Commission regularly consults individuals as well as organisations on a wide range of policy issues, while it develops the underlying policies. We have already outlined how the consultation process works in the case of research and innovation priorities in Horizon 2020.

4. **What are the provisions for the research budget for the future? What the emerging priorities areas?**

   It is difficult to discuss this question briefly for the whole of Horizon 2020. As we wrote above, Horizon 2020 can respond to emerging opportunities and needs. In the area of key enabling technologies, the general approach is to bring technologies closer to applications and the markets.

5. **Photochemistry can be used to solve the energetic problems of the EU. Does Europe favour this process? How?**

   Research and Innovation activities funded by ongoing and present Framework Programmes of the European Union are intensive in this field. Photochemistry does not show as an individual program but is covered in the industrial programmes. A search using " Photo-chemi*" on CORDIS

under projects (http://cordis.europa.eu/projects/home_en.html) gives 86 projects under the 7th Framework Programme (FP7). 34 under the previous FP6 and under FP5, 48. Using "Photo-cataly*" in the same searches gives FP7 (71), FP6 (12) and FP5 (11) projects. In the new EU Research and Innovation programme, Horizon 2020 (2014-2020), the calls are quite widely expressed and photochemistry could be part in many of the topics. The reason is that the method how to solve an issue is not specifically stated in the H2020 calls. The terms Photo-chemistry and Photo-catalysis are covered in a broader sense in the call "Innovative, Sustainable and inclusive Bioeconomy". An example is the topic ISIB-06-2015 "converting CO2 into chemicals". Furthermore the terms are also addressed under the "Call for Nanotechnologies, Advanced Materials and Production". Topic NMP-03-2015 is open for R&I activities for materials having bio-, photo- or thermo-chemical/physical properties. (Please also see the answer in question 6)

6. The transition towards the use of advanced materials for electronics needs an intensive development of the studies on the photoelectrochemical properties of these materials. What is the role of EU in this transition?

The European Commission has acknowledged the importance of Photonics by identifying it as a Key Enabling Technology for Europe. Europe should combine resources at all levels to significantly strengthen the sector. The challenge is both to lead in photonics technology innovation and to exploit these results though successful commercialisation. The EC has the influence, credibility and authority to act as the catalyst for setting the overall research agenda, harmonizing research programs with individual states, facilitating effective clustering of players, and avoiding fragmentation of efforts. The EU vision on "photonics" is addressed in the "European Technology Platform Photonics21" (http://www.photonics21.org/download/FinalEditionPhotonics21VisionDocument_InternetVersion.pdf) Horizon 2020 has for 2014 8 calls referring to "photonics".

http://www.spire2030.eu/uploads/Modules/Publications/spire-roadmap_december_2013_pbp.pdf

Both questions (5 and 6) are addressed under the SPIRE Roadmap. The Sustainable Process Industry through Resource and energy Efficiency (SPIRE) is a proposal for a Public Private Partnership (PPP) driven by the European Process Industry and fully aligned with the strategic goals defined by the European Commission in the Europe 2020 strategy. Here it is specifically stated that "generation of renewable energy through improved photovoltaic technology is also a requirement for success." (p.41)

Revisiting the Kasha Rule and the Heavy-Atom effect

Majed Chergui
Laboratoire de Spectroscopie ultrarapide, ISIC, FSB, Ecole Polytechnique Fédérale de Lausanne, CH-1015 Lausanne, Switzerland

Emission spectroscopy has been one of the most important tools for investigating energy redistribution in molecular excited states[1] ever since the birth of molecular spectroscopy at the beginning of last century. The many studies that followed thereafter led to the emergence of a number of general empirical rules of which two of the most important ones are:
(I) The Kasha rule, proposed in 1950[2], states that photon emission (fluorescence or phosphorescence) occurs in appreciable yield only from the lowest excited state of a given multiplicity. A corollary of Kasha's rule is the Kasha–Vavilov rule, which states that the quantum yield of luminescence is generally independent of the excitation wavelength.[3] This can be understood as a consequence of the tendency – implied by Kasha's rule – for molecules in upper states to relax to the lowest excited state non-radiatively.
(II) The heavy atom effect, which is defined by IUPAC as "The enhancement of the rate of a spin-forbidden process (if non-radiative, it is called intersystem crossing-ISC) by the presence of an atom of high atomic number, which is either part of, or external to, the excited molecular entity. Mechanistically, it responds to a spin-orbit coupling enhancement produced by a heavy atom."[4]
These rules were postulated well before the advent of the laser and in particular, of pulsed femtosecond lasers. The latter have represented a revolution for molecular spectroscopy as they enabled the study of phenomena occurring on the time scale of molecular vibrations. While the most commonly used technique is the pump-probe scheme, optical sampling methods such as fluorescence up- or down-conversion have been pushed into the femtosecond regime,[5-7] enabling detection of extremely short lived emission signals. Indeed, even for very short lived excited singlet states, there is a non-zero probability of emitting photons, which can be detected if the time window of the detection is adequately narrow. An important

improvement to the technique came with the introduction of CCD camera detectors coupled to a monochromator, allowing a polychromatic detection and therefore, bringing a significant increase in signal-to-noise and speed of data acquisition.[7-9] Figure 1 illustrates the capability of our set-up showing how the entire emission spectral profile can be recorded at each time delay.[10] In addition, we have extended its detection to the mid-IR[11] and to the UV around 300 nm.[12]

In this short review, we will mainly focus on our results from a combination of ultrafast and steady-state emission studies, and the way they allow us to revisit the above empirical rules in molecular photophysics.

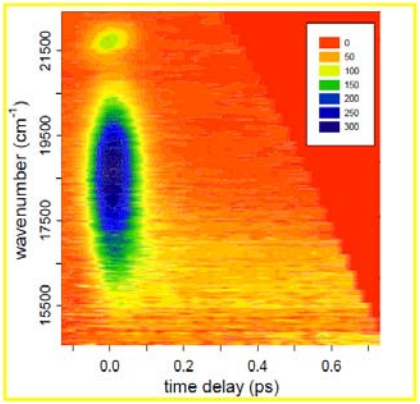

Figure 1. Emission of $[Ru(bpy)_3]^{2+}$ in water as a function of time upon excitation at 400 nm. The signal around t=0 between 16500 and 20000 cm^{-1} is due to the fluorescence of the singlet metal-to-ligand-charge-transfer (^{1}MLCT) state, while the yellow stripe centred around 16400 cm^{-1} is due to the ^{3}MLCT phosphorescence. The spot at 21600 cm^{-1} is the Raman band of the solvent.[10]

I. The Kasha rule:

I.a. Breaking the Kasha Rule: Few cases of the violation of the Kasha Rule exist, and a well-documented example was first reported in 1955 for azulene[13] and confirmed by more recent studies.[3,14] The classical explanation is that the S_1 and S_2 states lie sufficiently far apart that

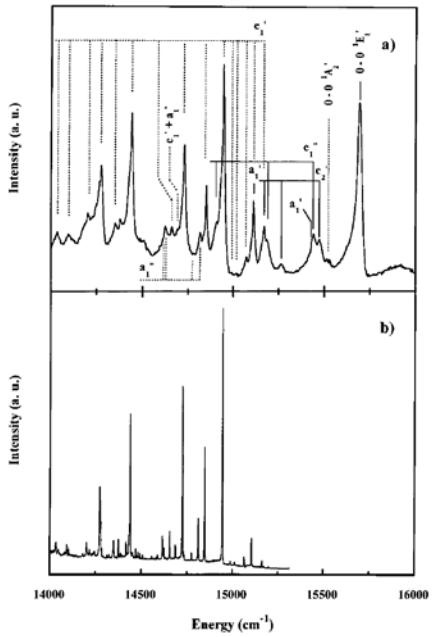

Figure 2. Fluorescence spectrum of C_{70} in solid neon for excitation at (a) 470 nm (21 277 cm^{-1}) above the S_2 state, and (b) 644.16 nm (15 524 cm^{-1}) at the electronic origin of the S_1 (S_0) transition, while dotted marks to those of the $^1E_1'(S_2)$-$^1A_1'(S_0)$ transition.[19,20]

fluorescence is observed mostly from S_2. Other examples concern the pyrenes[15,16] and naphthalene.[17,18] All these molecules are relatively small size polyatomics. As the number of degrees of freedom of the molecule increases and with it, the density of states, one expects the Kasha Rule to be more strictly observed.

At the end of the 1990s, we[19,20] reported on a striking violation of the Kasha Rule in the case of the C_{70} molecule trapped in neon matrices at low temperatures. As can be seen from figure 2a, fluorescence of both S_1 (A_2') and S_2 (E_1') states is observed for excitation at energies above the latter, while exciting the S_1 state yields only its own fluorescence (figure 2b). The transition between S_1 (A_2') and the singlet A_1' ground state is orbitally forbidden, but it can gain some

intensity via Herzberg-Teller coupling. On the other hand, S_2 (E_1') is dipole allowed to the ground state. Its fluorescence was attributed to the fact that it lies 165 cm^{-1} above the S_1 state, which is less than the smallest vibrational quantum of the molecule (~200 cm^{-1}) so that energy cannot be converted into vibrational energy of the molecule, thus creating a bottleneck to intramolecular non-radiative relaxation. This represents the largest molecule for which the Kasha Rule is violated.

I.b. Intermediate cases: As already mentioned, with improvements of the fluorescence up-conversion method, the ability to capture weak emission signals from higher lying states became possible. Over the past few years, we documented a number of cases, especially among coordination chemistry complexes, where emission from higher lying electronic states was observed.[21-23] The case of the Osmium complex $Os(dmbp)_3$ (dmbp= 4,4'-dimethyl-2,2'-biypridine) in ethanol[23] is clear-cut because we could detect an intermediate 50 ps lived emission, which is due to a higher triplet state lying at an energy ~2000 cm^{-1} above the lowest triplet state whose phosphorescence decays in 25 ns, due to a quantum yield of $\leq 5.0 \times 10^{-3}$.
The occurrence of such intermediate emissions imply that a weak proportion of population reaches the ground state bypassing the lowest electronic excited state. Although, they represent a violation of the Kasha-Vavilov Rule, it is a mild one. Indeed, if we assume a typical pure radiative lifetime of microseconds for the triplet state, it corresponds to an emission quantum yield of 10^{-6} for such states, and they would not be observable under steady-state detection conditions.

I.c Relaxation at sub-vibrational time scales: At the other extreme is the observation of a fluorescence that mirrors the absorption band of the lowest singlet state at the shortest time delays, i.e. within the pulse width of the pump laser, and regardless of the excitation energy. This is the case in figure 1 and is better depicted in Figure 3, which shows the absorption bands and the time-zero emission bands of $[Ru(bpy)_3]^{2+}$ and $[Fe(bpy)_3]^{2+}$ in solution. Similar observations were made on other Ru complexes[24] and were found to be independent of the solvent, symmetry of the complex and initially excited S_n state. The mirror profile of the emission implies that it occurs from a thermalized state, which seems paradoxical. The lowest singlet

fluorescence in Ru- and Fe-polypyridine complexes is found to be very short-lived (<40 fs).[24] In order to reach the S_1 state, the system has to relax the excess energy via electronic (internal conversion, IC) and vibrational levels (intramolecular vibrational redistribution, IVR). Taking its lifetime as an internal clock, this implies that the IVR/IC processes occur in < 10 fs,[24] i.e. on sub-vibrational time scales! It should however be stressed that thermalization is only with respect to the high frequency Franck-Condon modes that make up the modulations of the absorption band (figure 3). These dump their energy on a sub-vibrational time scale into the bath of low frequency, optically silent modes, in a fashion akin to a critically damped oscillator. When however, higher S_n states are excited, these very fast relaxation processes must occur in a strongly non-Born-Oppenheimer fashion for the IC, probably involving conical intersections between excited state potential surfaces. These results imply that IC/IVR within singlet states precedes ISC in these systems, contrary to previous claims based on monochromatic detection ultrafast fluorescence studies.[25,26]

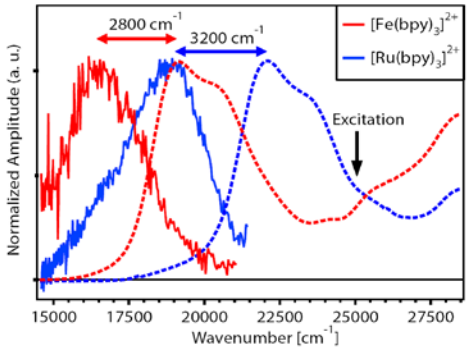

Figure 3: Steady-state absorption spectra showing the ^{1}MLCT absorption band (dashed traces) and time-zero fluorescence spectra of $[Fe(bpy)_3]^{2+}$ and $[Ru(bpy)_3]^{2+}$ in water, excited at 25000 cm^{-1} (black arrow). The horizontal arrows indicate the respective absorption-emission Stokes shift (from refs 10, 24 and 28).

The idea of dumping the energy into low frequency, optically silent modes is difficult to verify in the above examples because the singlet lifetime is too short, but we verified it in the case of organic dyes,

such as 2,5-diphenyloxazole (PPO) and para-terphenyl (pTP), pumped with a large excess of vibrational energy.[12,27] It was observed that at zero time delay, the mirror image of the fluorescence is already present but is structure-less. Thereafter, vibrational cooling of the low frequency modes and/or solvation dynamics occur on the time scale of several ps, which lead to a structured fluorescence spectrum, identical to the steady-state spectrum.

In conclusion, the observation of a mirror image fluorescence to the absorption of the lowest singlet state at the shortest time delay does not imply ultrafast cooling, except for the high frequency Franck-Condon modes, because the excess energy is redistributed into low frequency ones.

II. The heavy atom effect:
Figure 1 nicely illustrates the ability of the broad band fluorescence detection at fs resolution to observe the change from fluorescence to phosphorescence. In this case ($[Ru(bpy)_3]^{2+}$)[10] and in the case of a whole series of Ru- and Fe-polypyridine complexes,[24,28] the decay of the ^{1}MLCT (< 40 fs) fluorescence is reflected in the rise of the ^{3}MLCT state. Such ISC times are the shortest ever reported. Quite surprisingly, further investigations with heavier transition metal complexes did not deliver as short ISC times. Particularly noteworthy are two cases: a) the ISC rate between the lowest singlet and triplet states of a diplatinum complex (Pt_2POP) was found to lie in the 10-30 ps range and to be solvent-dependent![22]; b) In complexes such as $[Re(L)(CO)_3(bpy)]^{n+}$ (for L=Cl, Br, I, n=0; for L= Etpy= Ethylpyridine, n=1), the ISC times (100-150 fs) are significantly longer than in the Fe or Ru complexes, but remarkably, they decreased in the sequence I-Br-Cl, which is opposite to the trend expected from the "heavy-atom" effect. We also found a linear correlation between the ISC times and the Re-halogen stretch frequency for these complexes, suggesting that structural changes mediate the spin transition.
The comparison between the Fe, Ru, Pt, Re and Os complexes also underlines the importance of the density of states. For example, $Os(dmbp)_3$ showed slower ISC times than $Os(bpy)_2(dpp)$, which has a higher density of states.[23] A general discussion on the ultrafast ISC times reported for the above complexes and others is given in ref. [29].

Thus, the IUPAC[4] definition of the heavy atom effect needs to be revised. If a high spin-orbit coupling (SOC) constant is a necessary condition, it is not a sufficient one and other parameters, such as density of states, crossing of potential surfaces and even structural rearrangements play an important role. In a way, it is like in electron transfer reactions: a large driving force is necessary, but this does not mean an ultrafast electron transfer if the potential surfaces are weakly coupled or do not have the right crossings.

III. Outlook

The increased sensitivity of detection schemes for steady-state fluorescence allows the unravelling of new cases where the Kasha Rule is violated and we have presented the case of the largest ever molecule that violates it. The developments in ultrafast fluorescence spectroscopy also allow the detection of the emission from higher states with very low fluorescence yields. Finally, these new capabilities have opened the way to the systematic study of ISC in metal complexes, showing that it does not comply with the heavy atom effect. If a large SOC constant is necessary, this condition is not sufficient and density of states and structural considerations come into play in determining the ISC rate.

Our broadband fluorescence up-conversion is now routinely used to investigate the ultrafast dynamics of a wide range of different molecular, biological systems and nanosystems[11,30] in solutions. However, its full benefit lies in its combination with other tools, as was shown in the study of the photocycle of Fe(II) spin-cross over complexes, where it was combined with ultrafast X-ray[31] and optical transient absorption spectroscopy.[32] We also stressed the complementarity of the fluorescence up-conversion studies with transient absorption and photon echo studies.[33-35] More recently, with the development of 2-dimensional spectroscopy in the UV,[36,37] up-conversion in the UV becomes particularly attractive because of the complementarity between these two tools. In summary the combination of various experimental techniques allow us to harness the entire sequence of relaxation steps in polyatomic molecules, while at the same time delivering information about the photoinduced structural dynamics

References.

(1) Lakowicz, J. R. *Principles of fluorescence spectroscopy*; 3rd ed.; Springer: New York, 2006.
(2) Kasha, M. *Discuss Faraday Soc* **1950**, 14.
(3) Klán, P.; Wirz, J. *Photochemistry of organic compounds : from concepts to practice*; Wiley: Chichester, West Sussex, U.K., 2009.
(4) http://goldbook.iupac.org/H02756.html.
(5) Mokhtari, A.; Chesnoy, J.; Laubereau, A. *Chem Phys Lett* **1989**, *155*, 593.
(6) Arzhantsev, S.; Maroncelli, M. *Appl Spectrosc* **2005**, *59*, 206.
(7) Zhang, X. X.; Wurth, C.; Zhao, L.; Resch-Genger, U.; Ernsting, N. P.; Sajadi, M. *Review of Scientific Instruments* **2011**, *82*.
(8) Haacke, S.; Taylor, R. A.; Bar-Joseph, I.; Brasil, M. J. S. P.; Hartig, M.; Deveaud, B. *J Opt Soc Am B* **1998**, *15*, 1410.
(9) Zgrablic, G.; Voitchovsky, K.; Kindermann, M.; Haacke, S.; Chergui, M. *Biophysical Journal* **2005**, *88*, 2779.
(10) Cannizzo, A.; van Mourik, F.; Gawelda, W.; Zgrablic, G.; Bressler, C.; Chergui, M. *Angewandte Chemie International Edition* **2006**, *45*, 3174.
(11) Bonati, C.; Cannizzo, A.; Tonti, D.; Tortschanoff, A.; van Mourik, F.; Chergui, M. *Physical Review B* **2007**, *76*, 033304.
(12) Cannizzo, A.; Bram, O.; Zgrablic, G.; Tortschanoff, A.; Oskouei, A. A.; van Mourik, F.; Chergui, M. *Optics Letters* **2007**, *32*, 3555.
(13) Beer, M.; Longuethiggins, H. C. *J Chem Phys* **1955**, *23*, 1390.
(14) Wagner, B. D.; Tittelbachhelmrich, D.; Steer, R. P. *Journal of Physical Chemistry* **1992**, *96*, 7904.
(15) Geldof, P. A.; Rettschnick, R. P. H.; Hoytink, G. J. *Chem Phys Lett* **1969**, *4*, 59.
(16) Wannier, P.; Rentzepi.Pm; Jortner, J. *Chem Phys Lett* **1971**, *10*, 102.
(17) Wannier, P.; Rentzepi.Pm; Jortner, J. *Chem Phys Lett* **1971**, *10*, 193.
(18) Deinum, T.; Werkhove.Cj; Langelaa.J; Rettschn.Rp; Vanvoors.Jd *Chem Phys Lett* **1973**, *19*, 29.
(19) Sassara, A.; Zerza, G.; Chergui, M. *Journal of Physical Chemistry A* **1998**, *102*, 3072.
(20) Sassara, A.; Zerza, G.; Ciulin, V.; Portella-Oberli, M. T.; Ganiere, J. D.; Deveaud, B.; Chergui, M. *J Lumin* **1999**, *83-4*, 29.
(21) Cannizzo, A.; Blanco-Rodriguez, A. M.; El Nahhas, A.; Sebera, J.; Zalis, S.; Vlcek, A.; Chergui, M. *Journal of the American Chemical Society* **2008**, *130*, 8967.

(22) van der Veen, R. M.; Cannizzo, A.; van Mourik, F.; Vlcek, A.; Chergui, M. *Journal of the American Chemical Society* **2011**, *133*, 305.
(23) Bram, O.; Messina, F.; Baranoff, E.; Cannizzo, A.; Nazeeruddin, M. K.; Chergui, M. *J Phys Chem C* **2013**, *117*, 15958.
(24) Bram, O.; Messina, F.; El-Zohry, A. M.; Cannizzo, A.; Chergui, M. *Chem Phys* **2012**, *393*, 51.
(25) Bhasikuttan, A. C.; Okada, T. *J Phys Chem B* **2004**, *108*, 12629.
(26) Bhasikuttan, A. C.; Suzuki, M.; Nakashima, S.; Okada, T. *Journal of the American Chemical Society* **2002**, *124*, 8398.
(27) Braem, O.; Penfold, T. J.; Cannizzo, A.; Chergui, M. *Phys Chem Chem Phys* **2012**, *14*, 3513.
(28) Gawelda, W.; Cannizzo, A.; Pham, V. T.; van Mourik, F.; Bressler, C.; Chergui, M. *Journal of the American Chemical Society* **2007**, *129*, 8199.
(29) Chergui, M. *Dalton T* **2012**, *41*, 13022.
(30) Bonati, C.; Mohamed, M. B.; Tonti, D.; Zgrablic, G.; Haacke, S.; van Mourik, F.; Chergui, M. *Physical Review B* **2005**, *71*.
(31) Chergui, M. *Acta Crystallogr A* **2010**, *66*, 229.
(32) Cannizzo, A.; Milne, C. J.; Consani, C.; Gawelda, W.; Bressler, C.; van Mourik, F.; Chergui, M. *Coordin Chem Rev* **2010**, *254*, 2677.
(33) Oskouei, A. A.; Braem, O.; Cannizzo, A.; van Mourik, F.; Tortschanoff, A.; Chergui, M. *Chem Phys* **2008**, *350*, 104.
(34) Oskouei, A. A.; Tortschanoff, A.; Bram, O.; van Mourik, F.; Cannizzo, A.; Chergui, M. *J Chem Phys* **2010**, *133*.
(35) Ajdarzadeh, A.; Consani, C.; Bräm, O.; Tortschanoff, A.; Cannizzo, A.; Chergui, M. *Chem Phys* **2013**.
(36) Aubock, G.; Consani, C.; Monni, R.; Cannizzo, A.; van Mourik, F.; Chergui, M. *Review of Scientific Instruments* **2012**, *83*.
(37) Consani, C.; Aubock, G.; van Mourik, F.; Chergui, M. *Science* **2013**.

SPECIAL REPORTS ON FLUORESCENT SELF-ASSEMBLED NANO-OBJECTS

Introduction

Dear EPA members,

This issue of the EPA Newsletter, June 2014, is dedicated to "Fluorescent self-assembled nano-objects", which is currently a flourishing research area aimed at obtaining smart fully organic nanosystems and nanocomposites. We would like to thank the authors of the contributions to this issue of the EPA Newsletter for giving us an overview of their recent research. We are particularly grateful to Andre Del Guerzo who has also been the driving force for encouraging the other authors to contribute their work and submit it before the deadline.

An interesting collection of contributions related to fluorescent nanosystems is presented here. *Mireille Blanchard-Desce* (Institute of Molecular Science, University of Bordeaux) reports on the potential of biocompatible fully organic nanoparticles. Her group has succeeded in designing tuneable, hyper-bright, fully organic nanoparticles made of push-pull chromophores as biocompatible and non-toxic systems that are alternatives to quantum dots for bioimaging.

André Del Guerzo's (Institute of Molecular Science, University of Bordeaux) contribution focuses on the self-assembly of linear polyaromatic chromophores. His group proved for the first time that organic nano-fibers, which are transparent in the visible region, exhibit individual "white" emission. Interestingly, such emission is linearly polarized in the blue spectral region, but not in the orange/red spectral region. The potential of the self-assembly strategy for valuable materials is stressed.

Suzanne Fery-Forgues et al. (CNRS, University of Toulouse) report on the assembly of fluorescent organic dyes to give rise to injectable nanoparticles that offer numerous advantages compared to the dissolved dyes and dye-doped systems that are excitable at wavelengths appropriate for medical applications, and that exhibit low toxicity.

Ken Tsung Wong et al. (Department of Chemistry, National Taiwan University) report on the manipulation of fully organic photoactive

nanostructures. These structures comprise an electron rich - conjugated system capped at the end by biuret units, which impart the molecular recognition property that eventually results in the formation of the nanostructure. The researchers have designed systems which respond to light and/or solvent polarity thereby gaining insight into the basic ideas for the design of adaptive systems.
Rémi Métivier et al. (PPSM, ENS-Cachan, CNRS, France) focus their report on molecular assemblies combining photochromism and fluorescence, the preparation of organic nanoparticles based on photoswitchable fluorescent molecules, and the design of promising integrated photoactive multichromophoric systems as well as integrated multi-photoactive organic-inorganic hybrid nanomaterials.
Enrico Rampazzo and Damiano Genovese (Department of Chemistry, "G. Ciamician", University of Bologna) report on a direct micelle-assisted strategy with high molecular weight surfactants, such as Pluronic F127, to synthesize cross-linked micellar nanoparticles featuring fluorescent core-shell silica nanoparticles incorporating luminescent dyes. They have prepared PEG-capped luminescent silica nanoparticles as fluorescent probes. They have shown the cooperative action between the core and shell to increase the efficiency of the system and have succeeded in the preparation of near-infrared fluorescent nanoparticles for regional lymph node mapping.
Eléna Ishow et al. (PPSM-CNRS UMR, CEISAM-UMR CNRS, France) report on two strategies for the preparation of bimodal magnetic and fluorescent nanoassemblies. Fluorescence studies (steady-state and time-resolved) combined with TEM images are consistent with the formation of two different types of assembly depending on the method of preparation. One of the nanoassemblies comprises a pure organic core coated with supermagnetic iron oxide nanoparticles, whereas the other consists of a random mixture of fluorophores connecting maghemite nanoparticles.
Nathan D. McClenaghan (CNRS-University of Bordeaux, France) compares the photophysical properties of BODIPYs, which have been extensively studied, with those of less exploited analogues, namely AzaBODIPYs. This researcher foresees a promising future for the latter fluorophores, in particular when incorporated into functional nanomaterials targeting biomedical applications.
Albertus P. H. J. Schenning and Michael G. Debije (Department of Chemical Engineering and Chemistry, Eindhoven University of

Technology) report on the requirements that a fluorophore must fulfil to be used in luminescent solar concentrators, which are devices that can generate electricity from sunlight. An overview on the efforts already made to find such ideal fluorophores is presented; the researchers state that it remains a challenge.

Sajisha V. S. and Uday Maitra (Department of Organic Chemistry, Indian Institute of Science) report on the incorporation of lanthanide ions as structural components in cholate hydrogels as well as a doping of these supramolecular structures combined with small amounts of sensitizers. These researchers have recently devised a prosensitizer-based detection of enzymes strategy by using lanthanide cholate gel matrices.

The EPA Newsletter Board greatly appreciates these experts' contributions to this issue.

Julia Pérez Prieto
Associate Editor EPA Newsletter
Universidad de Valencia
Instituto de Ciencia Molecular (ICMol)
C/ Catedrático José Beltrán 2
46980 Paterna, Valencia

"Hyper-brigth" molecular-based fluorescent nanoparticles made from polar chromophores for bioimaging purposes: a bottom-up approach

Mireille Blanchard-Desce
Institute of Molecular Science, University of Bordeaux, 33405 Talence, France

In the last decades, inorganic nanoparticles have attracted growing attention in the field of nanophotonics, in relation with various applications including new imaging modalities. Among them luminescent metal- , semiconductor- or oxide based nanoparticles have been by far the most widely studied. Among them luminescent metallic and semiconducting nanoparticles have been heralded as major nanomaterials due to their unique electronic and optical properties, giving rise to the blooming field of plasmonics in the case of metallic nanoparticles. In parallel, semiconductor quantum dots have motivated many studies due to their unique electronic and optical properties. In particular their luminescence properties can be tuned in the visible-NIR region by playing on their size in relation with quantum confinement. However, a number of luminescent inorganic nanoparticules suffer from several drawbacks such as toxicity, blinking and raise a number of questions with respect to environmental issues (clearance, biodegradability…). Fully organic nanoparticles offer interesting potentialities and among them polymeric and self-assembled systems (nanosomes etc.) have received considerable attention. More recently, molecular-based fluorescent organic nanoparticles (FONs) have attracted increasing interest as they offer potential for a wide range of applications,[1] including biological applications.[2]

Key criteria for luminescent nanoparticles to be of interest for *bioimaging* purposes typically are large brightness (for enhanced sensitivity with single molecular imaging as an ultimate goal), photostability, colloidal stability as well as biocompatibility and (bio)degradability (and minimal toxicity). FONs may provide interesting alternatives to luminescent inorganic particles as their building blocks can be varied and meant to be non-toxic due to their intrinsically versatile structure. In that context, we have been interested in designing biocompatible FONS combining tunable

emission, huge brighthness (both for standard excitation i.e. confocal fluorescence microscopy, as well as for two-photon excitation i.e. two-photon laser-scanning microscopy), excellent colloidal and photo-stability in bioenvironments, aiming at various imaging modalities (including single particle tracking and two-photon imaging). To this aim, we have shown that subtle molecular engineering strategies of specific chromophoric subunits (namely push-pull chromophore, schematized as D-π-A in Fig. 1) represent successful bottom-up routes to such FONs. Original push-pull chromophores (Fig. 1) having thiophene units in the π-conjugated system - to allow efficient intramolecular charge transfer while preserving luminescence compared to their polyenic analogues - have been synthesized and FONs prepared using the simple precipitation method.[3] These push-pull chromophores were also selected as NLO-phores meant to display large nonlinear optical properties (both second-order[4] and third–order, including two-photon absorption properties[5]). The specificity of the implemented approach lies in the designed large dipolar character and polarizability of the chromophoric buiding blocks. These characteristics offer intriguing possibilities for the *control of luminescent properties by their molecular confinement* within organic nanoparticles (ONPs) due to strong interchromophoric dipole-dipole interactions (which influence molecular packing during the primary cluster formation processes) and resultant large *local electric fields* experienced by individual chromophoric subunits within ONPs (potentially leading to polarization effects). As an illustration of the potential of the manipulation of such effects, a striking enhancement and spatial confinement of luminescence has been achieved in fully organic core-shell nanoparticles made from dedicated complementary push-pull dyes, due to the generation of large electric fields at the core-shell nano-interface.[6] Another fascinating outcome of the specific nature of dedicated push-pull chromophoric subunits is the large FONs surface potential they generate.

Figure 1. Molecular engineering of push-pull chromophores for the design of bright FONs with tunable emission and improved colloidal stability

Indeed molecular engineering of the push-pull chromophoric subunits allows both tuning the luminescence properties and influencing colloidal stability. This makes the FONs made such chromophroic subunits quite different from those made from seminal chromophores generally used in the preparation of "classical" FONs reported in the literature (typically aromatic derivatives). The large local electric fields generated when such chromophores are brought into close proximity play a dual role: they influence both the organization of chromophoric subunits within the FONs (via dipole-dipole interactions) and their luminescence properties (via modulation of their electronic gap). Hence both the electronic properties (dipole moment, polarizability etc.) and the geometry of chromophoric subunits (including charge distribution) are expected to play a significant role in molecular confinement-induced effects. As a striking example of this phenomenon, FONs made from dipolar chromophore **1** (**FONs1**) are found to be strong green emitters whereas FONs made from its three-branched octupolar analogue **1'** are weaker orange emitters (Table 1).[7] In addition, whereas **FONs1** show sufficient colloidal stability and were demonstrated to be non-toxic contrast agents of major interest for *in vivo* angiography in small animals, **FONs1'** were found to rapidly form micro-agglomerates after intra-cardiac injection in Xenopus laevis tadpoles.[7] These microaggregates deposit in the tiny blood

vessels, hindering blood flow and causing subsequent lethal occlusion of the blood vessels. Hence the nature of the chromophoric subunits has major effects on surface properties and colloidal stability of resulting FONs. This opens interesting potentialities as the FONs surface potential is thus expected to be modulated by playing on the chemical nature of the push-pull subunits constituting the FONs. This was successfully achieved by a simple engineering of the dipolar chromophoric subunit. Indeed the extension of the π-conjugated system (i.e. by going from "naked" dipolar chromophore **1** to "naked" dipolar chomophore **2**) allows both red-shifting **FONs2** emission while maintaining fluorescence and significantly increasing their colloidal stability in water.[8] This simple bottom-up strategy led to bright orange-emitting FONs that combine enhanced colloidal stability in water and giant one-and two-photon brightness (Table 1).

Table 1. Characteristics of FONs made from different push-pull chromophores and their one- ($\varepsilon^{max}\Phi$) and two-photon brightness ($\sigma_2^{max}\Phi$)

cpd	R [a] (nm)	λ_{abs}^{max} (nm)	λ_{em}^{max} (nm)	Φ [b] %	$\varepsilon^{max}\Phi$ (10^8 $M^{-1}cm^{-1}$)	σ_2^{max} [c] (10^6 GM)	$\sigma_2^{max}\Phi$ (10^6GM)
1	17	418	538	15	1.3	5	0.8
1'	17	422	582	2	0.2	8	0.2
2	18	422	597	7	0.6	8	0.55
3	40	560	800	2	0.2	-	-

[a] Mean radius of the nanoparticles (derived from TEM)
[b] Fluorescence quantum yield in deionized water
[c] Two-photon absorption cross-section per nanoparticle (derived from TPEF experiments)

Further extending this bottom-up approach (Fig. 1), push-pull chromophores bearing different and stronger electron-withdrawing groups (to engineer the surface potential and tune the fluorescence emission in the visible-NIR region) and suitable elongated π-conjugated connector (to increase colloidal stability) were prepared (such as dipolar chromophore **3** in Fig. 1). This led to Hyper-bright NIR-emitting FONs (which we named HiFONs) that combine *narrow* emission (thus competing with QDs), *remarkable* chemical and colloidal stability in water (and in biological environments as well as in saline buffer or varying pH conditions).[9] Strikingly these HiFONS

show both improved chemical stability and photostability as compared to isolated chromophores in aqueous environments, showing that molecular confinement of custom-designed chromophores is an intriguing strategy. HiFONs were also shown to display excellent biocompatibility with no observed toxicity, thus providing superior alternatives to QDs for bioimaging purposes.[9] Thanks to their remarkable stability and outstanding NIR brightness (typically 3 orders of magnitude larger than those of prototypical water-soluble NIR emitting dyes), HiFONs were successfully imaged at single particles level after 24 hour integrating into cellular environments and demonstrated to allow single particle tracking in water (Fig. 2).

Figure 2. Single particle imaging in COS cells (left) and single particle tracking (right) of NIR-emitting HiFONS made from dedicated push-pull chromophore **3** (middle) in water (from ref.9).

The bottom-up approach based on molecular engineering of polar and polarizable chromophores has thus proven of major potential for bioapplications, already leading to biocompatible, ultra-bright and (photo)stable fully organic nanoparticles that fully compete with inorganic QDs. HiFONs constitute a new class of biocompatible luminescent nanotools of foremost promises. In particular imparting recognition features through suitable chemical functionalization would allow HiFONs to be targeted to various receptors and proteins, to reveal the dynamic secrets of biomolecules in NIR range by single particles imaging and tracking.

Acknowledgements.
Conseil Régional d'Aquitaine is gratefully acknowledged for financial support (Chaire d'Accueil grant to MBD).

References.

1. Patra, A.; Chandaluri, C. G.; Radhakrishnan, T. P. *Nanoscale* **4**, 343-359 (2012) and references cited therein.
2 Fery-Forgues, S. *Nanoscale* **5**, 8428-8442 (2013) and references cited therein.
3. Nakanishi, H.; Oikawa, H. in Single Organic Nanoparticles; Masuhara, H.; Nakanishi, H.; Sasaki, K. (Ed.), Springer-Verlag: Berlin. 2003; pp 17-31.
4. Batista, R. M. F.; Costa, S. P. G.; Belsley, M.; Lodeiro, C.; Raposo, M. M. M. *Tetrahedron* **64**, 9230-9238 (2008).
5. Genin, E.; Hugues, V.; Clermont, G.; Herbivo, C.; Castro, M. C. R.; Comel, A.; Raposo, M. M. M.; Blanchard-Desce, M. *Photochem. Photobiol. Sci.* **11**, 1756-1766 (2012).
6. Campioli, E.; Rouxel, C.; Campanini, M.; Nasi, L.; Blanchard-Desce, M.; Terenziani, F. *Small* **9**, 1982-1988 (2013).
7. Parthasarathy, V.; Fery-Forgues, S.; Campioli, E.; Recher, G.; Terenziani, F.; Blanchard-Desce, M. *Small* **7**, 3219-3229 (2011).
8. Amro, K.; Daniel, J.; Clermont, G.; Bsaibess, T.; Pucheault, M.; Genin, E.; Vaultier, M.; Blanchard-Desce M. *Tetrahedron* **70**, 1903-1909 (2014).
9. Genin, E.; Gao, Z.; Varela, J. A.; Daniel, J.; Bsaibess, T.; Gosse, I.; Groc, L.; Cognet, L.; Blanchard-Desce M. *Adv. Mater.* **26**, 2258-2261 (2014).

In Search of the Ideal Fluorophore for Luminescent Solar Concentrators

Albertus P.H.J. Schenning, Michael G. Debije
Laboratory of Functional Organic Materials and Devices, Department of Chemical Engineering & Chemistry, Eindhoven University of Technology, 5600 MB Eindhoven, The Netherlands

Luminescent solar concentrators (LSCs) are essentially simple devices that could be used to generate electricity from sunlight in urban settings (see Fig. 1).[1] Generally they consist of a plastic lightguide filled or topped by fluorescent dyes. The dyes absorb incident sunlight and re-emit it at a longer wavelength. A fraction of the emitted light is trapped in the high refractive index lightguide and escapes via the edges of the plates, where one may place long, thin photovoltaic (PV) cells to generate electrical power. The LSC could be employed where silicon is not appropriate, because the LSC may be colourful, of any shape, and works in cloudy and shaded conditions.

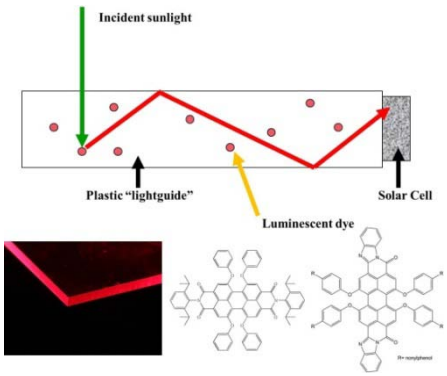

Figure 1. (Top) Function of LSC. (Bottom) Photograph of an LSC illuminated from above by UV light demonstrating the edge emission from the lightguide; chemical structures of Red305 and perylene perinone [2].

The single most important aspect of the LSC is the dye molecule. There are several requirements for this fluorophore: it must absorb in

the correct part of the solar spectrum, it must have a very high fluorescent quantum yield, demonstrate photostability, and a large Stokes shift is desired. The most common dyes used in LSCs are perylenes. However, these dyes often show sparing solubility and limited Stokes shift, which results in reabsorption of emission light which can be lost either by non-unity fluorescent yields, or emission from the top of bottom surfaces.

We have employed a perylene perinone dye to extend the absorption spectra by 50 nm, and in so doing gain access to 25% more photons than the most commonly use dye in LSCs, the perylene based Lumogen Red305 from BASF.[2] However, the solubility remains modest and the fluorescent yield is not optimal. Another challenge is to generate dye molecules that give blue and yellow color to the plastic plates, which aides in architectural integration, because these dyes tend to degrade too quickly in sunlight. Inorganic materials have also been considered, but these have their own limitations: for example, phosphors have too low an absorption coefficient and require such high doping concentrations they cause scatter of waveguiding light, and quantum dots often suffer from efficiency and lifetime issues.

So, the challenge remains. Significant advances in the performance of LSCs have been realized in the past few years by application of concepts such as dye alignment[3] and control of light loss through surfaces.[4] Efficiencies have improved with devices providing appreciable efficiencies,[5] and the first applications are beginning to be seen in the built environment. But until the fluorescent molecule is improved, the LSC will be restricted in use and performance, and it is clear that the discovery of this elusive fluorophore should be at the forefront of future LSC research.

References

1. Debije, M.G., Verbunt, P. P. C. *Adv. Energ. Mater.* **2**, 12-35 (2012).
2. Debije, M.G., Verbunt, P. P. C., Nadkarni, P.J., Velate, S., Bhaumik, K., Nedumbamana, S., Rowan, B.C., Richards, B.S., Hoeks, T. *Appl. Optics* **50**, 163-169 (2011).
3. Verbunt, P.P.C., Kaiser, K., Hermans, K., Bastiaansen, C.W.M., Broer, D. J., Debije, M.G. *Adv. Func. Mater.* **19**, 2714-2719 (2009).
4. Debije, M.G., Van, M.-P., Verbunt, P.P.C. Kastelijn, M.J., van der Blom, R.H.L., Broer, D.J., Bastiaansen, C.W.M, *Appl. Optics* **49**, 745-751(2010.); Goldschmidt, J.C., Peters, M., Bösch, A., Helmers,

H., Dimroth, F., Glunz, S.W., Willeke, G.P., *Sol. Energ. Mater. Sol. C.* **93**, 176-182 (2009).
5. Slooff, L.H., Bende, E.E., Burgers, A.R., Budel, T., Pravettoni, M., Kenny, R.P., Dunlop, E.D., Büchtemann, A., *Phys Status Solidi - R* **2**, 257-259 (2008); Desmet, L., Ras, A.J.M., De Boer, D.K.G., Debije, M.G., *Opt. Lett.* **37**, 3087-3089 (2012).

Light-Emitting Self-Assembled Nano-Fibers

André Del Guerzo
Nanostructures Organiques, Institut des Sciences Moléculaires, CNRS UMR 5255
Université de Bordeaux, 33400 Talence, France

The dense organization of chromophores into nanostructures can pave the way for a variety of applications in the fields of photonics, opto-electronics, photo-catalysis and photo-patterning. The method that is presented here relies on the self-assembly of modified chromophores providing nano-fibers or nano-ribbons. In the first case, the interweaving of nano-fibers during their growth can result in the trapping of the solvent and the formation of a soft material, a thermally reversible organogel.

In the last decade, we have focused on the use of linear polyaromatic chromophores, called acenes, comprising well-known compounds such as anthracenes, tetracenes and pentacenes. The modification of these in the axial positions 2,3 with long alkyloxy chains induces their self-assembly into nano-fibers (~80-150 nm wide) and organogels. Detailed studies have been performed on the super-gelator 2,3-didecyloxyanthracene (DDOA). It was shown by X-ray scattering (SAXS) and crystallographic studies that the anthracene derivatives are highly ordered in the nanofibers (on a tens of nanometer scale).[1] However, a certain degree of disorder and highly anisotropic kinetics of self-assembly inhibit the formation of large crystals and lead to the formation of these *quasi*-unidimensional structures.

DDOA nanofibers are fluorescent in the blue spectral region, with a quantum yield of 24% when DMSO is the solvent of the gel (almost the same Φ_{em} as in chloroform solution).[2] This indicates that, in contrast to what is often observed in dense aggregates of chromophores, there are no strong quenching processes prevailing in these nanostructures. Further detailed studies have revealed that a DDOA to DDOA exciton hopping mechanism occurs in the nanofibers. A combination of this mechanism and Förster energy transfer can be exploited to sensitize 2,3-dialkoxy-substituted tetracenes doped into these nanofibers.[2,3] The control of the relative

proportions of energy donor (DDOA) and acceptor (tetracene, 0 - 2 *%equivalents*) can be exploited to fine-tune the color of the emission of the nanofibers.

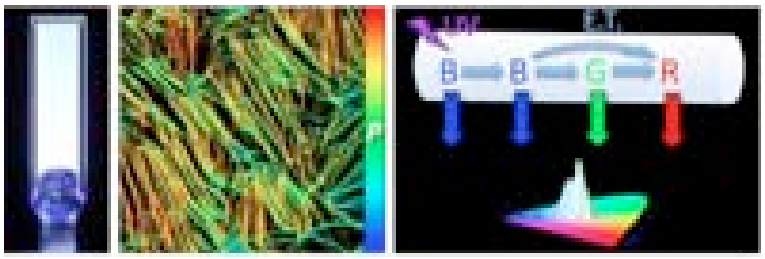

Figure 1. *(left to right)* Photo under UV-light of a white-light emitting organogel. Confocal fluorescence polarization microscopy image of the same gel in the blue spectral region. Schematic representation of the photophysical mechanism occurring in a single nanofiber. Distribution of CIE coordinates of the emission of individual nanofibers (~hundred 20 μm long segments of them).[2]

In a recent study, DDOA has been co-assembled with 2,3-dihexadecyloxy derivatives of diphenyltetracene and rubrene (tetraphenyltetracene) in order to achieve color-tuneable emission including white-light (Fig. 1). In the latter case, a confocal fluorescence microscopy study has been essential to reveal the characteristics of the photophysical processes and insights on the co-assembly of three chromophores.[2] Indeed, it was shown that each nanofiber of the organogel homogeneously emits white-light. This was the first case proven on individual "white" nano-fibers. Moreover, fluorescence lifetime imaging (FLIM) has shown that the energy transfer mechanism occurs efficiently in all the fibers. Confocal fluorescence polarization microscopy has also revealed a particularity: the emission of "white" nanofibers is linearly polarized in the blue spectral region, whereas it is not in the orange/red spectral region. Thus, these nano-objects display the rare property of polarization-dependent emission color. Furthermore, these polarization images provide important insights on the self-assembly

of acenes in the nanofibers: *(i)* the DDOA matrix is highly organized leading to linearly polarized emission (in agreement with X-ray studies); *(ii)* both the diphenyltetracene and the rubrene derivative disperse well in the fiber network, but, in contrast to diphenyltetracene, the rubrene derivative displays a random orientation leading to unpolarized emission. This information is unique in order to understand the co-assembly and could not be obtained otherwise, since rubrene is present only at 1.2 *%equivalents* in the nanofibers.

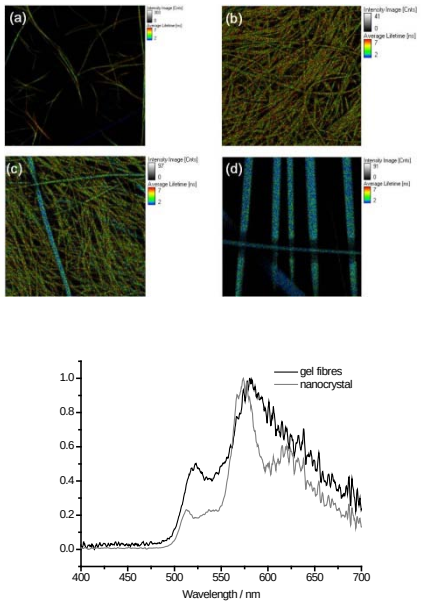

Figure 2. *(up)* FLIM Fluorescence lifetime images (a: 4040 μm; b,c,d: 3030 μm) of 3 mM DDPEA in *n*-butanol at *r.t.*, λ_{ex} 375 nm, λ_{em} 405 nm (color code: average decay time): (a) solvated gel fibers; (b) non-aged sample air-dried; (c) aged for 2hr and then dried; (d) aged for 4hr and then dried. *(bottom)* Spectra of fibers (black, areas similar to sample (b)) and ribbons (grey, areas similar to sample (d)) obtained by confocal micro-spectroscopy.[4]

More recently, 2,3-disubstituted anthracenes have been modified also in the meso position 9,10 with phenyls or ethynylphenyls. This leads to a strengthening of the lowest energy optical transition that occurs along the short axis of the aromatic core. These derivatives display very high quantum yields that can reach 95% in solution in the blue spectral region. 2,3-dihexadecyl-9,10-diethynylanthracene (DDPEA) self-assembles in organic solvents, but differs from the previously mentioned DDOA by two main aspects.[4] First, the emission occurs from J-aggregates, as revealed by the strong red-shift in absorption and emission. This drastic spectroscopic change is related to a different molecular packing in the self-assembled state and a larger oscillator strength in DDPEA leading to a stronger intermolecular dipolar coupling. Second, we observed by confocal microscopy that the morphology of the self-assembled state evolves over a few hours. Indeed, the initially formed nanofibers ripen and become larger nano-ribbons with slightly different spectroscopic and photophysical properties (Fig. 2). Similarly, diphenylanthracene derivatives can yield nano-ribbons that display exceptional properties. They combine high emission quantum yields, spectral tunability and very high linear polarization of the emission.

In conclusion, we can assert that the self-assembly of alkoxy-substituted acenes is a successful strategy to obtain fluorescent anisotropic nano-objects with interesting optical properties: transparency in the visible region, tuneable fluorescence in the visible including white light, and linear polarization of the emission. The exploitation of self-assembly also opens up to other opportunities: alignment of nanofibers on a macroscopic scale,[5] induction of optical chirality by co-assembly,[6] and formation of composite materials including inorganic nanoparticles.[7]

References.

1. Terech, P.; Aymonier, C.; Loppinet-Serani, A.; Bhat, S.; Banerjee, S.; Das, R.; Maitra, U.; Del Guerzo, A.; Desvergne, J.-P. *J. Phys. Chem. B* **114**, 11409-11419 (2010).
2. Giansante, C.; Raffy, G.; Schäfer, C.; Rahma, H.; Kao, M.-T.; Olive, A.G.L.; Del Guerzo, A. *J. Am. Chem. Soc.* **133**, 316-325 (2011).
3. Giansante, C.; Schäfer, C.; Raffy, G.; Del Guerzo, A. *J. Phys. Chem. C* **116**, 21706-21716 (2012).
4. Kao, M.-T.; Schäfer, C.; Raffy, G.; Del Guerzo, A. *Special Issue in honor of J.-P. Desvergne, Photochem. Photobiol. Sci.* **11**, 1730-1736 (2012).
5. Shklyarevskiy, I.O.; Jonkheijm, P.; Christianen, P.C.M.; Schenning, A.P.H.J.; Meijer, E.W.; Del Guerzo, A.; Desvergne, J.-P.; Maan, J.C. *Langmuir* **21**, 2108-2112 (2005).
6. Banerjee, S.; Das, R.K.; Terech, P.; de Geyer, A.; Aymonier, C.; Loppinet-Serani, A.; Raffy, G.; Maitra, U.; Desvergne, J.-P.; Del Guerzo, A. *J. Mater. Chem. C* **1**, 3305-3316 (2013).
7. Das, R.K.; Bhat, S.; Banerjee, S.; Aymonier, C.; Loppinet-Serani, A.; Terech, P.; Maitra, U.; Raffy, G.; Desvergne, J.-P.; Del Guerzo, A. *J. Mater. Chem.* **21**, 2740-2750 (2011).

Luminescent Lanthanide Cholate Hydrogels

*Sajisha V. S. and Uday Maitra**
Department of Organic Chemistry, Indian Institute of Science, Bangalore-12, India

The extraordinary luminescence properties of lanthanide ions has been a theme of active research owing to their applications in chemistry, biology and material science.[1] The classical method of complexing lanthanide ions with suitable ligands to give strong emission suffers from drawbacks such as laborious synthetic steps and unpredictable efficiency of the ligands. Though the compartmentalization of lanthanide ions along with sensitizers in an anionic micelle to enhance the luminescence was known[2] as early as 1977, the area remained almost untouched thereafter.

In this context we came up with the idea of incorporating lanthanide ions as a structural component in the cholate hydrogel matrices. We have shown that doping these supramolecular gels with minute quantities (μM) of the sensitizers [e.g., pyrene for europium and 2,3-dihydroxynaphthalene (DHN) for terbium] resulted in enhanced luminescence. Energy transfer from Tb(III) to Eu(III) was also explored in the hydrogel matrix allowing us to make colour tunable gels and luminescent coating materials.[3] Later, we have also succeeded in sensitizing Tb(III) in deoxycholate *organogel* matrix using DHN, and demonstrated selective quenching of luminescence by electron poor polyaromatic hydrocarbons.[4]

More recently, we have utilized the lanthanide cholate gel matrix containing nano fibres as a common platform for developing simple and efficient "*pro*-sensitizer" based sensing and assay of various enzymes.[5] The fact that protected DHN derivatives (diacetoxy DHN or DHN glucoside) failed to sensitize Tb(III) prompted us to use them as "*pro*-sensitizers" which upon the action of enzymes (lipase and β-glucosidase, respectively) released the sensitizer (DHN) thus enhancing Tb(III) luminescence. The enhancement in the Tb(III) luminescence allowed us to develop a rapid enzyme sensing and assay technique.

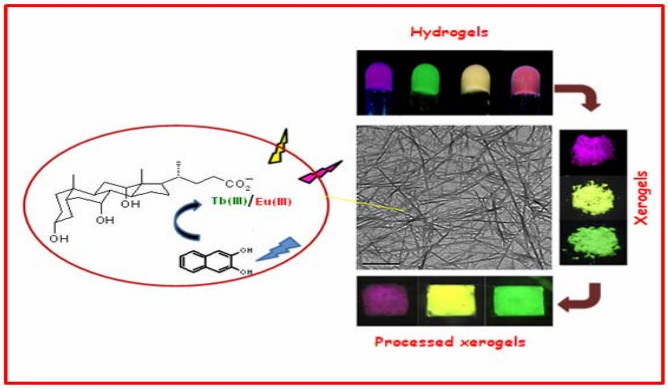

Colour tunable gels/coating materials

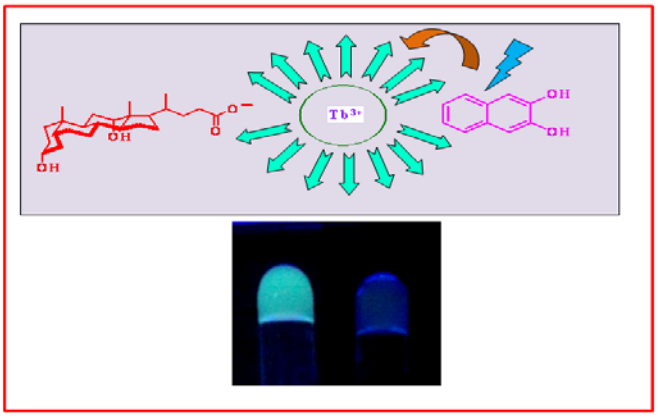

Detection of electron poor polyaromatic hydrocarbons

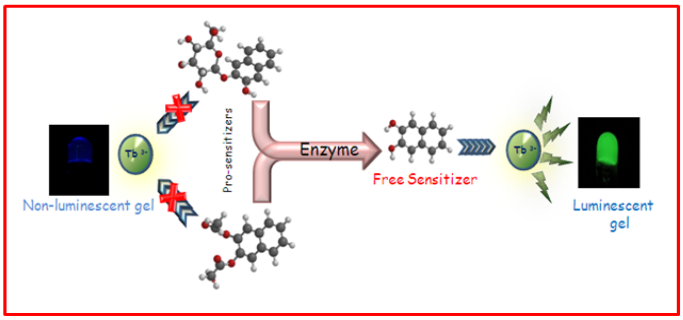

Enzyme sensing and assay

Figure 1. A schematic representation of the applications of luminescent lanthanide cholate/deoxy cholate gels

1. Binnemans, K. *Chem. Rev.* **109**, 4283 (2009).
2. Perez, J. R.; Nome, F.; Fendler, J. H. *J. Am. Chem. Soc.* **99**, 7749 (1977).
3. (a) Bhowmik, S.; Banerjee, S.; Maitra, U. *Chem. Commun.* **46**, 8642-8644 (2010) (b) Banerjee, S.; Kandanelli, R.; Bhowmik, S.; Maitra, U. *Soft Matter* **7**, 8207-8215 (2011).
4. Kandanelli, R.; Sarkar, A.; Maitra, U. *Dalton Trans.* **42**, 15381-15386 (2013).
5. Bhowmik, S.; Maitra, U. *Chem. Commun.* **48**, 4624-4626 (2012).

High density bimodal magnetic and fluorescent nanoparticles as potential biomaging agents

*Gaëlle Prével,[1] Adrien Faucon,[2] Marie Breton,[1] Jean-Frédéric Audibert,[1] Jérôme Fresnais,[3] Jean-François Berret,[4] Julie Hémez,[2] Eric Gautron,[5] Eléna Ishow[1,2]**

[1]PPSM-CNRS UMR 8531, Ecole Normale Supérieure de Cachan, 94235 Cachan Cedex, France

[2] CEISAM–UMR CNRS 6230, Université de Nantes, 44322 Nantes, France.

[3] PECSA-UMR CNRS 7195, Université Pierre et Marie Curie, 75005 Paris, France.

[4]MSC-UMR CNRS 7057, Université Paris Diderot, 75013 Paris, France.

[5] IMN–UMR CNRS 6502, Université de Nantes, 44322 Nantes, France

The development of highly sensitive and non-invasive techniques to probe biological mechanisms and address cell dysfunction has recently boosted the fabrication of multifunctional nanoparticles.[1] In this context, the combination of magnetic and luminescent entities represents considerable interest.[2] First, remote orthogonal stimuli (light or magnetic field) whose intensity and energy are easily modulated can be used to address the nanoparticles. Secondly, dyes emitting in distinct spectral regions can be combined and independently visualized to provide multiplexed detection.[3] Thirdly, magnetic components impart the assemblies with potentialities of collective migration, tissue imaging by resonance magnetic imaging and cell therapy by hyperthermia, by applying an external static or alternative magnetic field.[4] While the emissive units involve mostly organic dyes or quantum dots (QDs), the magnetic units are exclusively made of inorganic entities where iron oxide nanoparticles are regarded as privileged materials due to the absence of significant cytotoxicity.[5] Therefore, the association of both kinds of units requires careful elaboration to keep the functionalities intact. Two main strategies have been adopted, namely blends of magnetic and fluorescent entities as dopants of silica nanoparticles,[6] and coating of magnetic nanoparticles with emissive units.[7] Such coating can be realized through covalent linkage of the organic dyes or QDs or by entrapping the emissive units in thin polymer[8] or silica shell[8a, 9] around the magnetic core. For both strategies, inherent dilution of

the dyes occurs, which leads to a decrease in the emission intensity. Recently, fluorescent organic nanoparticles (FON), composed of semi-conjugated polymers[10] or small molecules,[11] have emerged to give high signal-to-noise ratios in bioimaging[12] and minimize progressive photobleaching upon optical investigation. Surprisingly, their combination to magnetic nanoparticles has rarely been considered.

We have recently explored the strategy of using FON as central platforms of magnetofluorescent hybrid assemblies.[13] In this way, novel core-shell architectures consisting of a fluorescent core[14] coated with a layer of superparamagnetic iron oxide nanoparticles (*fluo@mag*) could be obtained (Fig. 1).

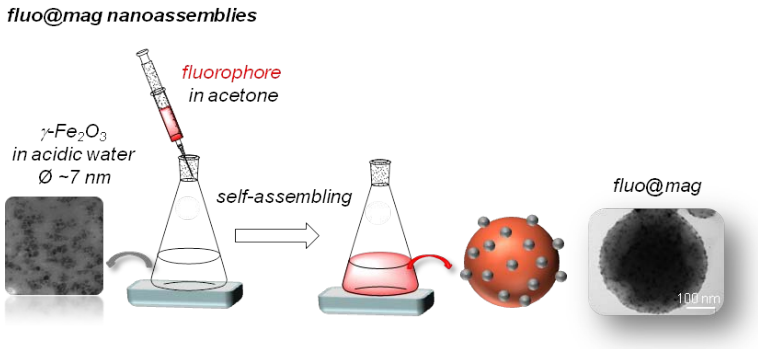

Figure 1. Schematic description of the assembling process for the bimodal nanoassemblies *fluo@mag*.

The surrounding inorganic layer advantageously protect the organic core from interacting with the aqueous medium, which could lead to emission quenching or color shift in case of changes in polarity, viscosity, ionic strength or pH. Moreover, the high density of fluorophores, larger than 10^5 dyes per nanoparticle, leads to brightness similar to that of QDs. The nanoassembly fabrication results from the quick injection of a concentrated solution of hydrophobic dyes (here 4-di(4'-*tert*-butylbiphenyl-4-yl)amino-4'-dicyanovinylbenzene),[15] prepared in pre-filtered acetone or tetrahydrofuran, into an acidic suspension of 7 nm-wide maghemite γ-Fe_2O_3 nanoparticles, issued from iron salt coprecipitation and

oxidation.[16] Dye nanoreprecipitation as nanospheres occurs and is followed by self-assembling of inorganic nanoparticles at the organic nanosphere surface. Such self-assembling is driven by electrostatic or iono-covalent interactions depending on the fluorophore architectures. In order to avoid emission reabsorption by the magnetic layers, fluorophores with significant charge transfer conducting to red-shifted emission, need to be employed. Surface potential measurements of organic nanoparticles in our case always reveal negatively charged surface. The surface potential ζ, valued between -30 and -40 mV, was ascribed to either partial ionization of the introduced iron-chelating functions (like phosphonic and carboxylic acids),[17] or to strong polarization of water molecules and/or interface adsorption of carboxylate ions, present as common contaminants in water.[18] In all cases, transmission electron microscopy (TEM) imaging revealed a "raspberry-like" architecture. They however questioned the possible presence of iron oxide nanoparticles inside the organic core during the self-assembling process. Ultracryomicrotomy attempts and TEM imaging failed to evidence pure organic nanocores, circled with iron oxide nanoparticles to assert the exclusion of maghemite nanoparticles from the core.

It turns out that fluorescence lifetime imaging microscopy appeared as an attractive and simple tool to gain insight into the nanoassembly structure. Iron oxide nanoparticles actually quench the emission of most fluorophores due to fast photoinduced electron transfer. The exponential distance dependence of electron transfer could indeed provide useful information about the structure of composite materials.

To have elements of comparison, we elaborated a second kind of architecture, dubbed *fluo@mag*, privileging intermixed γ-Fe_2O_3 nanoparticles and organics. To this aim, we used 10 nm wide hydrophobic γ-Fe_2O_3 nanoparticles, coated with Beycostat NE (BNE) ligands that are surfactants composed of a complex mixture of mono- and di-esters of phosphoric acids containing aryl and ethylenoxy units.[19] The iron oxide nanoparticles were then mixed with an organic solution of the same fluorescent dyes as those involved in the *fluo@mag* architectures (Fig. 2).

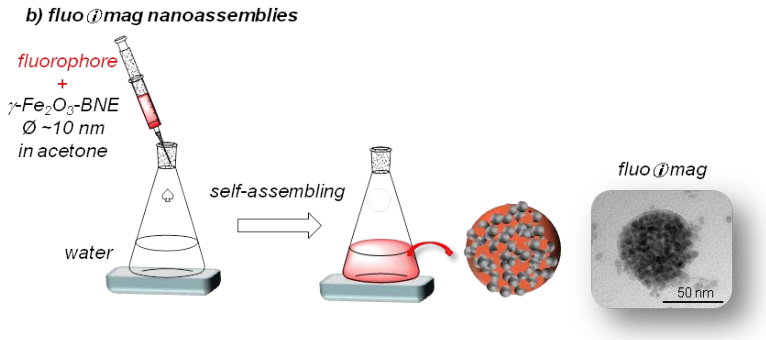

Figure 2. Schematic description of the assembling process for the bimodal nanoassemblies *fluo⦶mag*.

Quick addition of small aliquots (100 µL) of the resulting mixture into Millipore water (5 mL) yielded novel nanoassemblies, emitting at 630 nm under optical excitation (against 650 nm for the *fluo@mag* nanoassemblies) and migrating in the presence of a permanent magnet. Their morphology investigated by TEM imaging also slightly differed from the *fluo@mag* one and looks like quite intermixed organic and maghemite materials. Dynamic light scattering measurements of the *mag⦶fluo* nanoassemblies revealed a diameter increase of the nanoassemblies (from 180 nm up to 700 nm) with increasing ratios of magnetic NPs to fluorophores (from 10:1 to 30:1). This behavior is opposite to what was observed for the *fluo@mag* structures whose size decreased (from 180 nm down to 35 nm) with larger amounts of magnetic NPs (1 to 100-fold amount in excess to the dyes). Since the dyes do not form micelles or vesicles, encapsulation of higher amounts of maghemite nanoparticles was ruled out as a possible explanation of the growth of the nanoassemblies.

Time-resolved fluorescence investigations were performed to point out the structural differences between *fluo@mag* and *fluo⦶mag* nanoassemblies, using an excitation at 513 nm and an inverted fluorescence microscope equipped with a 40× air objective (N.A. 0.6). The fluorescence decay $I(t)$ could be modeled by a biexponential mathematical law $a_1\exp(-t/\tau_1) + a_2\exp(-t/\tau_2)$ where a_i and τ_i represent the pre-exponential factor and associated time constant

respectively. A longer τ_1 and a shorter τ_2 time constants were found with almost equal normalized fractional amplitudes f_1 and f_2 defined as $f_i = a_i / \sum_j a_j$. Compared to previous studies performed on FON constituted of fluorophores only, the longer lifetime τ_1 can be attributed to a core component while the shorter lifetime τ_2 is related to the surface component. For *fluo@mag* nanoparticles, the time constants τ_1 and τ_2 were considerably reduced for increasing concentrations of maghemite nanoparticles (Fig. 3a).

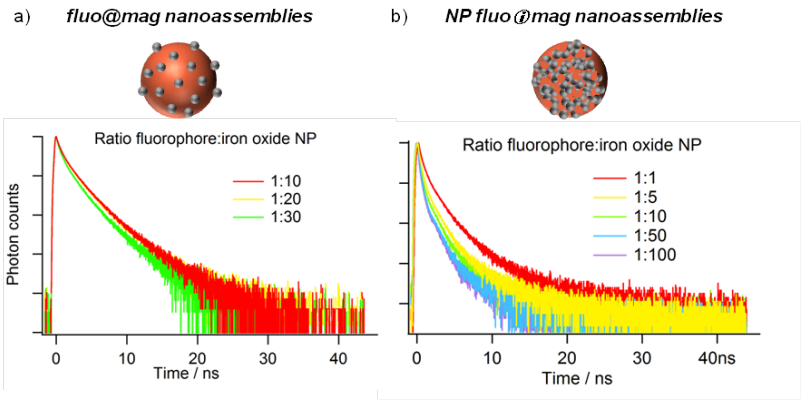

Figure 3. Evolution of the fluorescence decays as a function of the ratio fluorophore:iron oxide NP for the bimodal nanoassemblies *fluo@mag* and *fluo@mag* after excitation at 513 nm using an inverted fluorescence microscope equipped with time-resolved fluorescence facility (see ref.[14] for more details).

Their values evolved from 2.0 ns down to 1.0 ns for τ_1, and from 0.6 ns down to 0.2 ns for τ_2 in the range of investigated concentrations of γ-Fe_2O_3 nanoparticles. This contrasts with the *fluo@mag* nanoparticles whose global lifetime is much less affected (Fig. 3b). We indeed found that τ_1 shortened from 2.6 ns to 2.0 ns only while τ_2 changes from 1.0 ns down to 0.6 ns when the relative amount of γ-Fe_2O_3 nanoparticles increased by a threefold factor. Similar evolutions were noted for steady-state fluorescence measurements that showed much stronger diminution of the

fluorescence signal for *fluo@mag* compared to *fluo@mag* nanoparticles with an increasing amount of iron oxide nanoparticles. Such behaviors can be interpreted through a static fluorescence quenching mechanism combined to possible electron transfer as already mentioned. If the thickness for the magnetic layer around the organic core is assumed to be constant for one given *fluo@mag* nanoassembly, a smaller organic core leads to shorter distances between the internal organic and the external inorganic units. Hence, enhanced quenching efficiency and shorter time constants would be observed for smaller *fluo@mag* nanoparticles, and agree with the experimental observations. By contrast, for *fluo@mag* nanoassemblies, the lesser influence of the maghemite nanoparticle concentration indicates quite constant surroundings around each fluorophore. A slight 20 nm hypsochromic shift of the emission signal was actually detected for *fluo@mag* compared to *fluo@mag* nanoassemblies. This recalls the polarity dependence of the emission signal of the fluorophores, resulting from restricted torsions of their molecular backbone in less polar media.[20] We can thus reasonably assume direct contact of the fluorophores with the BNE ligands' surroundings. All these observations tend to suggest that the fluorophores would act as gluing material and assemble the superparamagnetic nanoparticles through van der Waals interactions in an intermixed structure *fluo@mag*. Hence, bigger nanoassemblies could form in the presence of larger amounts of iron oxide nanoparticles.

From these steady-state and time-resolved fluorescence studies, we can reasonably conclude that the *fluo@mag* nanoassemblies comprise a pure organic core coated with iron oxide nanoparticles whereas the *fluo@mag* nanoassemblies are made of a random mixture of fluorophores bridging maghemite nanoparticles. Both architectures illustrate direct and simple self-assembling processes which permit straightforward change in the functional units to yield bimodal nano-objects, adapted to the targeted bioimaging studies.

References.

1. (a) Cheon, J.; Lee, J. H. *Acc. Chem. Res.* **41**, 1630-1640 (2008); (b) Pelaz, B.; Jaber, S.; de Aberasturi, D. J.; Wulf, V.; Aida, T.; de la Fuente, J. M.; Feldmann, J.; Gaub, H. E.; Josephson, L.; Kagan, C.

R.; Kotov, N. A.; Liz-Marzán, L. M.; Mattoussi, H.; Mulvaney, P.; Murray, C. B.; Rogach, A. L.; Weiss, P. S.; Willner, I.; Parak, W. J. *ACS Nano* **6**, 8468-8483 (2012); (c) De, M.; Ghosh, P. S.; Rotello, V. R. *Adv. Mater.* **20**, 4225-4241 (2008); (d) Lee, J. E.; Lee, N.; Kim, T.; Kim, J.; Hyeon, T. *Acc. Chem. Res.* **44**, 893-902 (2011).
2. (a) Kim, J.; Piao, Y.; Hyeon, T. *Chem. Soc. Rev.* **38**, 372-390 (2009); (b) Josephson, L.; Kircher, M. F.; Mahmood, U.; Tang, Y.; Weissleder, R. *Bioconjugate Chemistry* **13**, 554-560 (2002).
3. Vendrell, M.; Zhai, D. T.; Er, J. C.; Chang, Y. T. *Chem. Rev.* **112**, 4391-4420 (2012).
4. (a) Lartigue, L.; Hugounenq, P.; Alloyeau, D.; Clarke, S. P.; Levy, M.; Bacri, J. C.; Bazzi, R.; Brougham, D. F.; Wilhelm, C.; Gazeau, F. *ACS Nano* **6**, 10935-10949 (2012); (b) Yoo, D.; Lee, J. H.; Shin, T. H.; Cheon, J. *Acc. Chem. Res.* **44**, 863-874 (2011).
5. Reddy, L. H.; Arias, J. L.; Nicolas, J.; Couvreur, P. *Chem. Rev.* **112**, 5818-5878 (2012).
6. (a) Salgueiriño-Maceira, V.; Correa-Duarte, M. A.; Spasova, M.; Liz-Marzán, L. M.; Farle, M. *Adv. Funct. Mater.* **16**, 509-514 (2006); (b) Insin, N.; Tracy, J. B.; Lee, H.; Zimmer, J. P.; Westervelt, R. M.; Bawendi, M. G. *ACS Nano* **2**, 197-202 (2008).
7. Bertorelle, F.; Wilhelm, C.; Roger, J.; Gazeau, F.; Ménager, C.; Cabuil, V. *Langmuir* **22**, 5385-5391 (2006).
8. (a) Di Corato, R.; Bigall, N. C.; Ragusa, A.; Dorfs, D.; Genovese, A.; Marotta, R.; Manna, L.; Pellegrino, T. *ACS Nano* **5**, 1109-1121 (2011); (b) Shi, D. L.; Cho, H. S.; Chen, Y.; Xu, H.; Gu, H. C.; Lian, J.; Wang, W.; Liu, G. K.; Huth, C.; Wang, L. M.; Ewing, R. C.; Budko, S.; Pauletti, G. M.; Dong, Z. Y. *Adv. Mater.* **21**, 2170-2171 (2009).
9. (a) Yang, H.; Zhuang, Y.; Hu, H.; Du, X.; Zhang, C.; Shi, X.; Wu, H.; Yang, S. *Adv. Funct. Mater.* **20**, 1733-1741 (2010); (b) Abou-Hassan, A.; Bazzi, R.; Cabuil, V. *Angew. Chem. Int. Ed.* **48**, 7180-7183 (2009).
10. (a) Wu, C.; Bull, B.; Szymanski, C.; Christensen, K.; McNeill, J. *ACS Nano* **2**, 2415-2423 (2008); (b) Wu, C.; Schneider, T.; Zeigler, M.; Yu, J.; Schiro, P. G.; Burnham, D. R.; McNeill, J. D.; Chiu, D. T. *J. Am. Chem. Soc.* **132**, 15410-15417 (2010).
11. (a) Cui, Q. H.; Zhao, Y. S.; Yao, J. *Adv. Mater.* DOI: 10.1002/adma.201305913, (2014); (b) Zhao, Y. S.; Fu, H.; Peng, A.; Ma, Y.; Xiao, D.; Yao, J. *Adv. Mater.* **20**, 2859-2876 (2008); (c) Petkau,

K.; Kaeser, A.; Fischer, I.; Brunsveld, L.; Schenning, A. *J. Am. Chem. Soc.* **133**, 17063-17071 (2011).
12. (a) Gole, A.; Stone, J. W.; Gemmill, W. R.; zur Loye, H.-C.; Murphy, C. J. *Langmuir* **24**, 6232-6237 (2008); (b) Parthasarathy, V.; Fery-Forgues, S.; Campioli, E.; Recher, G.; Terenziani, F.; Blanchard-Desce, M. *Small* **7**, 3219-3229 (2011).
13. Faucon, A.; Fresnais, J.; Brosseau, A.; Hulin, P.; Nedellec, S.; Hemez, J.; Ishow, E. *J. Mater. Chem. C* **1**, 3879-3886 (2013).
14. Breton, M.; Prevel, G.; Audibert, J. F.; Pansu, R.; Tauc, P.; Le Pioufle, B.; Francais, O.; Fresnais, J.; Berret, J. F.; Ishow, E. *Phys. Chem. Chem. Phys.* **13**, 13268-13276 (2011).
15. Ishow, E.; Brosseau, A.; Clavier, G.; Nakatani, K.; Tauc, P.; Fiorini-Debuisschert, C.; Neveu, S.; Sandre, O.; Leaustic, A. *Chem. Mater.* **20**, 6597-6599 (2008).
16. Massart, R.; Dubois, E.; Cabuil, V.; Hasmonay, E. *J. Magn. Magn. Mater.* **149**, 1-5 (1995).
17. Faucon, A.; Lenk, R.; Hemez, J.; Gautron, E.; Jacquemin, D.; Le Questel, J.-Y.; Graton, J.; Brosseau, A.; Ishow, E. *Phys. Chem. Chem. Phys.* **15**, 12748-12756 (2013).
18. Roger, K.; Cabane, B. *Angew. Chem. Int. Ed.* **51**, 5625-5628 (2012).
19. Da Cruz, C.; Sandre, O.; Cabuil, V. *J. Phys. Chem. B* **109**, 14292-14299 (2005).
20. Ishow, E.; Guillot, R.; Buntinx, G.; Poizat, O. *J. Photochem. Photobiol. A: Chem.* **234**, 27-36 (2012).

Photoswitchable fluorescent molecules and nanosystems

Rémi Métivier,[1] Jonathan Piard,[1] Karima Ouhenia-Ouadahi,[1] Stéphane Maisonneuve,[1] Jia Su,[1] Corentin Pavageau,[1] Jean-Pierre Placial,[1] Arnaud Brosseau,[1] Juan Xie,[1] Pei Yu,[2] Keitaro Nakatani[1]*
(1) PPSM, ENS-Cachan, CNRS, 61 av Pdt Wilson, F-94235 Cachan cedex, France. E-mail: metivier@ppsm.ens-cachan.fr.
(2) ICMMO, Univ. Paris-Sud, 15 rue Clémenceau, F-91405 Orsay cedex, France.

The development of novel optical devices, such as light-driven optical memories or biocompatible nanophotoswitches for super-resolution imaging, attracts considerable interest in the growing field of photoresponsive nanotechnologies.[1] We report here on the design of fluorescent photoswitchable materials, based on photochromic and fluorescent molecules.

Photochromic compounds are excellent candidates for such applications as they show the required properties for rewritable optical storage or photoswitchable probes: the transition between the two isomers A and B, corresponding to different absorption spectra, can be reversibly induced reversibly by ultra-violet (UV) or visible illumination.[2] The use of photochromic molecules, although attractive, is however limited by the fact that the color change of the macroscopic materials requires the switching of a very large number of molecules. Consequently, such a situation contributes to a slow response of the macroscopic device and reduces its applicability. To take full advantage of the photoswitching ability of the photochromic compounds, it turns necessary to increase significantly the sensitivity to determine the state of the system. Therefore, a key objective of our research is to implement fast and efficient photoswitchable systems by a sound combination of photochromism with fluorescence.

Indeed, the detection techniques based on fluorescence are extremely sensitive, and the use of fluorescence to probe the state of matter becomes widespread in various fields of science (biology, environment, materials...). Numerous examples of molecules based on a photochromic moiety associated to a fluorophore have been

reported in the literature over the last decade. In these systems, the fluorescence intensity detected when the photochromic unit is in the state A, for example, is turned "off" when the photochromic is in the state B. Three main types of molecular assemblies combining photochromism and fluorescence may be envisaged (Figure 1):[3]

- Type 1: photochromic and fluorescent moieties are not covalently linked. For example, an intermolecular resonance energy transfer (or photoinduced electron transfer) must be able to quench efficiently the fluorophore when the photochromic molecule is in its state B. The fluorescence must be restored when the photochromic derivative returns back to its state A.

- Type 2: photochromic and fluorescent units are covalently linked in a so-called "dyad" molecule. Intramolecular as well as intermolecular energy (or electron) transfer processes are expected to take place. An alternative of this type of assembly consists in a covalent grafting of the two units on the same platform (cyclodextrins, nanoparticles...).

- Type 3: photochromic molecules may themselves show fluorescence properties, whose characteristics are different in state A and B. No transfer process is required, though intermolecular energy transfer can be considered.

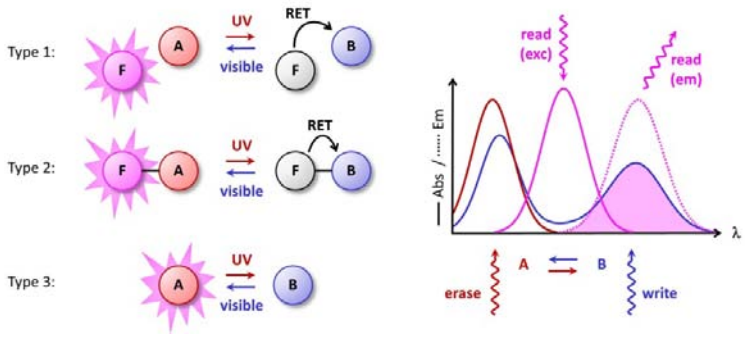

Figure 1. Schematic description of three types of fluorescent and photochromic molecular assemblies, for example based on a resonance energy transfer (RET). Activation and deactivation of the fluorescence is controlled through the photochromic species (write/erase), whereas probing the state of the system if performed by excitation of the fluorophore (read).

As a first example of the "type 1" combination of photochromism and fluorescence, we incorporated a diarylethene compound (P_1) and a commercial fluorophore (F_1) in a polymer matrix. These dyes have been selected such that the spectral overlap between the fluorescence spectrum of the fluorophore and the absorption spectrum of the closed form of the diarylethene (P_1-CF) is as large as possible (Figure 2a).

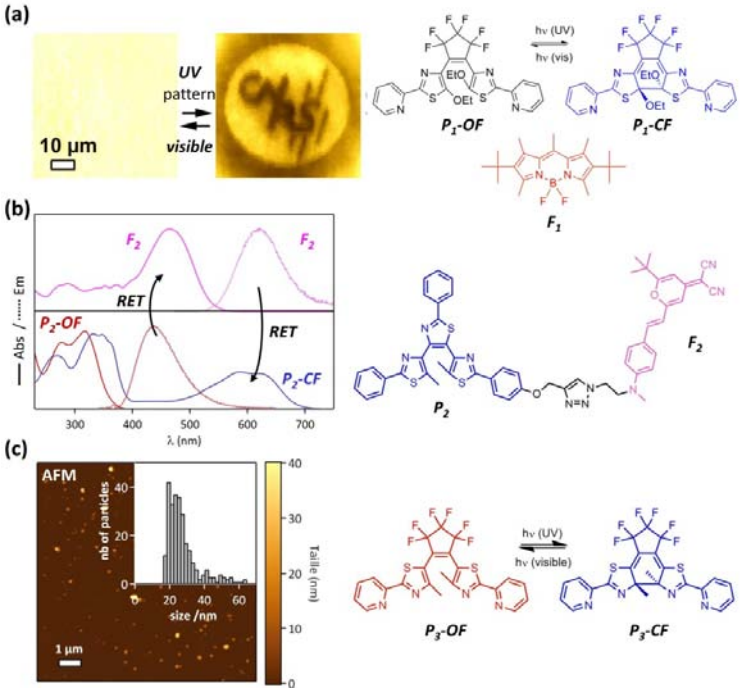

Figure 2. (a) Reversible 2D-pattern writing and erasing experiments in a polymer film doped with a diarylethene (P_1) and a fluorophore (F_1). (b) Bi-directional resonance energy transfer in a covalent photochromic-fluorescent (P_2-F_2) molecular dyad. (c) Photochromic-fluorescent organic nanoparticles of P_3.

In this way, an efficient energy transfer is expected from the fluorophore to the photochromic molecule in its closed form

($F_1 \rightarrow P_1$-CF), while no transfer occurs when the diarylethene is in its open form (P_1-OF). Thin PMMA films containing P_1 and F_1 compounds in varying concentrations were prepared by spin coating onto glass coverslips. UV light irradiation of the samples induces almost complete quenching of the fluorescence. The fluorescence is fully restored under visible irradiation. A large number of successive of UV and visible irradiation cycles has shown the possibility to modulate the fluorescence of the samples without any degradation of their properties. Write-read-erase experiments of a 2D-pattern under microscope have been carried out on the scale of a few micrometers (Figure 2a).[4]

We also implemented the strategy of the "type 2" association of photochromic and fluorescent properties. Covalent coupling at the molecular level has been realized between two moieties by "click chemistry": a photochromic terthiazole diarylethene compound (P_2) and a dicyanomethylene derivative (F_2) (Figure 2b). The photochromic unit is colorless in its open form (P_2-OF) and slightly emissive in the blue. Its fluorescence spectrum overlaps the absorption spectrum of the fluorophore, thus allowing a P_2-OF$\rightarrow F_2$ energy transfer. In contrast, the photochromic moiety in its closed form (P_2-CF) is colored with an absorption spectrum which overlaps the red emission band of the fluorophore, leading to an efficient energy transfer from the fluorophore to the closed-form of the diarylethene $F_2 \rightarrow P_2$-CF. We have successfully identified and quantified these bi-directional energy transfer processes between the photochromic unit and the fluorophore by steady-state and time-resolved fluorescence investigations in acetonitrile solution: $\Phi_{P2\text{-}OF \rightarrow F2} = 0.85$; $\Phi_{F2 \rightarrow P2\text{-}CF} \sim 1$.[5]

Finally, we designed organic nanosystems of the "type 3", composed of intrinsically fluorescent photochromic molecules. In this regard, the reverse diarylethene P_3 appears particularly promising (Figure 2c). Indeed, it shows effective photochromic properties but extremely weak fluorescence in solution, whereas in the solid state, this material exhibits an intense fluorescence but no photochromic activity. Therefore, this compound is not suitable for fluorescence photoswitching, neither in solution nor in solid state. Then, we decided to prepare organic nanoparticles by the laser ablation method. An aqueous suspension of P_3 nanoparticles, containing an anionic surfactant (sodium dodecyl sulfate, SDS) was obtained and

characterized by AFM and DLS, with sizes between 20 and 30 nm. Interestingly, the nanoparticles show intermediate photophysical properties, halfway between the solid state and the solution state. Indeed, from the solution to the colloidal suspension and the solid state, the ratio of the cyclization *vs.* ring-opening quantum yields ($\Phi_{P3\text{-}OF \rightarrow P3\text{-}CF}$ / $\Phi_{P3\text{-}CF \rightarrow P3\text{-}OF}$) decreases until it reaches zero in the solid state (no photochromism). On the contrary, the fluorescence quantum yield, almost negligible in solution ($<10^{-4}$), increases noticeably in the nanoparticles state (~0.02) and reaches a rather high value in the solid state (~0.2). Thus, nanoparticles of P_3 show both photochromic and fluorescence properties, which can be advantageously exploited for fluorescence photoswitching applications: under UV illumination, the fluorescence signal decreases by 60 %, and several UV-visible irradiation cycles can be realized without degradation of the properties of the system.[6]

As a conclusion, a wide variety of photochromic-fluorescent molecular systems has been successfully obtained, from doped polymer materials to molecular dyads and organic nanoparticles. Fluorescence photoswitching properties have been demonstrated, and quantified in terms of intermolecular and/or intramolecular resonance energy transfer. New promising perspectives can be envisioned in terms of photoactive multichromophoric systems[7] or hybrid organic-inorganic nanostructures.[8]

References.

1. Feringa, B. L. Molecular Switches; Wiley-VCH: Darmstadt (2001).
2. Irie, M. *Chem. Rev.*, **100**, 1683-1890 (2000), *special issue*.
3. Fukaminato, T. *J. Photochem. Photobiol. C*, **12**, 177-208 (2011).
4. Métivier, R.; Badré, S.; Méallet-Renault, R.; Yu, P.; Pansu, R.; Nakatani, K. *J. Phys. Chem. C*, **113**, 11916-11926 (2009).
5. Ouhenia-Ouadahi, K.; Métivier, R.; Maisonneuve, S.; Jacquart, A.; Xie, J.; Léaustic, A.; Yu, P.; Nakatani, K. *Photochem. Photobiol. Sci.*, **11**, 1705-1714 (2012).
6. Piard, J.; Métivier, R.; Giraud, M.; Léaustic, A.; Yu, P.; Nakatani, K. *New J. Chem.*, **33**, 1420-1426 (2009).
7. Maisonneuve, S.; Métivier, R.; Yu, P.; Nakatani K.; Xie, J. *Beil. J. Org. Chem.* (2014), *in press*.
8. Ouhenia-Ouadahi, K.; Yasukuni, R.; Yu, P.; Laurent, G.; Pavageau, C.; Grand, J.; Guérin, J.; Léaustic, A.; Félidj, N.; Aubard, J.;

Nakatania, K.; Métivier, R. *Chem. Commun.* (2014), DOI: 10.1039/c4cc02179g.

From BODIPYs to AzaBODIPYs: Versatile photostable fluorophores and tagged nanoparticles

Nathan D. McClenaghan
Institut des Sciences Moléculaires, CNRS-University of Bordeaux, France

The rapid evolution of fluorescence and microscopy imaging techniques has exerted more exacting criteria on the performance of emissive dyes and nanomaterials, leading to a renaissance in synthetic functional dye development. One versatile class of fluorescent dye which has received particular attention is the BODIPY family (see examples **1** and **2** in Fig. 1a), which comprises a dipyrromethene, which typically complexes a BF_2 unit.[1] The IUPAC name for the BODIPY core is 4,4-difluoro-4-bora-3a,4a-diaza-s-indacene.

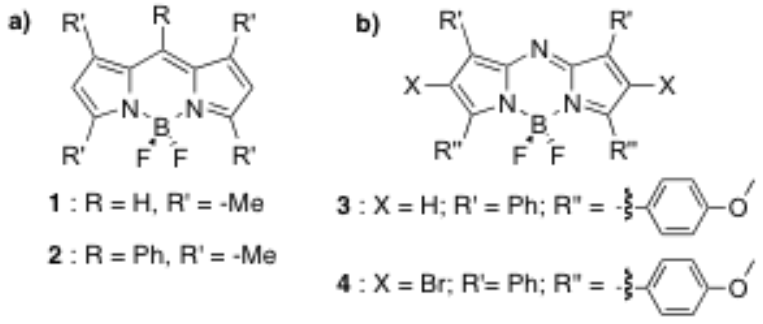

Figure 1. Generic structural formulas of BODIPY (a) and AzaBODIPY dyes (b).

The emergence of these dyes is related to their synthetic accessibility, elevated absorption and high emission quantum yields (which can tend to 1), and which are relatively insensitive to the environment, except in specific cases. Colour-tuning emission from the visible

towards the NIR therapeutic window can be achieved on synthetically-extending the conjugation of the emissive core. Indeed, a range of elaborate architectures have been developed harnessing this strategy, as well as multichromophore variants, which are of particular interest for light harvesting implementations. On the downside, photostability of BODIPYs, while high, is typically similar to fluorescein (photodegradation quantum yield = circa 10^{-5}) and extending conjugation to obtain NIR absorbing and emitting variants may compromise the final chemical and photochemical stability.[2]

A promising, less well-known, alternative to the BODIPY framework can be obtained upon replacing the *meso*-carbon with a nitrogen atom, giving rise to what are often referred to as AzaBODIPYs, and more appropriately named azadipyrromethenes, again BF_2-complexing variants being the more abundant species (see examples **3** and **4** in Fig. 1b). Here this minimalist structural variation has a tremendous impact on several of the key parameters. Notably, the absorption and emission wavelengths of BF_2-azadipyrromethenes are significantly red-shifted with respect to analogous BODIPYs. For example, molecule **3** has absorption and emission maxima at 682 nm and 721 nm, respectively, permitting NIR excitation and emission detection without recourse to extend the π-conjugated backbone, which may hamper certain other properties. In terms of application in imaging, brightness (taken as a product of molar extinction coefficient and the emission quantum yield) is somewhat lower for AzaBODIPYs as the emission quantum yields are typically lower (e.g. 0.4 for **3**) while similarly intense absorption can be noted, and their fabrication can necessitate extra synthetic steps compared with BODIPYs, which can in certain cases be prepared in a one-pot procedure. However, a second attractive feature for practical implementation of AzaBODIPYs is an extremely high photostability.[3] Recent ensemble measurements on **3** in air-equilibrated solution show the photodegradation quantum yield to be $< 10^{-8}$, some 3-orders of magnitude lower than typical BODIPYs and perhaps among the most photostable organic dyes known.

This combination of inherent red light absorption and high photostability are extremely promising for applications in live imaging, as well as photodynamic therapy (PDT). Indeed, incorporating heavy atoms such as bromine in the *β*-position (e.g. **4**) promotes intersystem crossing to a triplet state (with a quantum yield

of *ca.* 0.7) giving an efficient sensitizer for singlet oxygen production. Preclinical tests on these promising PDT agents are ongoing.

Beyond the properties of the BF_2-azadipyrromethene molecules themselves, some unique fluorescence switching properties have been recently observed in chromophore-nanoparticle (NP) hybrids.[4] This has been exemplified by surface grafting of an analogue of **3** onto 200 nm polymer beads. Due to the propensity of the tetraaryl derivatives to stack, as well as strong surface interactions, dramatic fluorophore quenching results. Upon endocytosis into living cells, the fluorescence is restored, leading to an effective real-time probe of cell internalization of NPs due to a strong fluorescence contrast of intra- and extracellular species. Fluorescence switching "on" is ascribed to deaggregation of the surface-bound fluorophores via formation of a phospholipid envelope around the hybrid NP, which is supported by in *vitro* experiments and fluorescence lifetime distribution analysis.[4]

In conclusion, NIR-addressable and photostable azadipyrromethenes constitute an underexploited class of dye for applications in imaging and therapy. New synthetic approaches and derivatives warrant investigation, as well as incorporation into functional nanomaterials for biomedical applications, assuring that azadipyrromethene dyes will enjoy a bright future.

References.

1. Loudet, A.; Burgess, K. *Chem. Rev.* **107**, (11): 4891–4932 (2007).
2. Vives, G.; Giansante, C.; Bofinger, R.; Raffy, G.; Del Guerzo, A.; B. Kauffmann, B.; Batat, P.; Jonusauskas, G.; McClenaghan, N. D. *Chem. Commun.* **47**, 10425-10427 (2011).
3. Batat, P.; Cantuel, M.; Jonusauskas, G.; Scarpantonio, L.; Palma, A.; O'Shea, D. F.; McClenaghan, N. D. *J. Phys. Chem A*, **115**, 14034–14039 (2011).
4. a) Palma, A.; Alvarez, L. A., Scholz, D.; Frimannsson, D. O.; Grossi, M.; Quinn, S. J.; O'Shea, D. F. *J. Am. Chem. Soc.* **133**, 19618-19621 (2011); b) McClenaghan, N.; O'Shea, D.; Jonusauaskas, G.; Esposito, R. et al. in preparation.

Manipulations of photoactive nanostructures

*Monima Sarma and Ken-Tsung Wong**
Department of Chemistry, National Taiwan University
No. 1, Sec. 4, Roosevelt Rd. Taipei 10617, Taiwan, E-mail:kenwong@ntu.edu.tw

The morphology of nanostructures self-assembled from tailor-made molecules is generally administered by the balance between various non-covalent interactions, of which hydrogen bonds (H-B) take a special note because of their directional nature. Among various structural motifs coding for H-B, biurets are known to be an excellent H-B functional group. For the first time, a versatile building block (**1**) incorporating the desired unprotected biuret unit was devised to smoothly introduce the aryl biuret group to the electron rich π-conjugated systems by the Suzuki–Miyaura coupling method.[1] The biuret-end-capped π-conjugated systems impart molecular recognition properties that result in the formation of distinct nanostructures depending on the structural features of the π–conjugated cores. For example, the blue fluorescent bifluorene-cored molecule (**2**) can self-assemble into a globular structure, whereas the green fluorescent bis(styryl)phenylene-centered molecule (**3**) can form a fibrous structure. Upon blending the donor molecule **2** with acceptor **3** (10% w/w), the formation of interdispersed nano network phases were observed, in which Förster resonant energy transfer (FRET) between them is highly efficient. [1] The structure of the self-assembled aggregates from molecule **2** was further characterized by SEM, TEM, and AFM to be vesicle-like hollow structure.[2] Results from dynamic light scattering (DLS), cryogenic-scanning electron microscopy and small-angle X-ray scattering experiments revealed that the aggregates are present in THF solutions.[3] However, switching the solvent from THF to DMSO, a solvent that is known to break up H-B interactions, will lead to the disappearance of the DLS signal. This finding proves that H-B interactions between biurets are crucial for aggregation. The solid-state structure of the phenylbiuret (**1**) indicated that the two-dimensional intermolecular H-B imparted by the biuret group had an important function in governing the formation of ribbons.[4] In the case of molecule **2** containing two biuret units, the intermolecular H-

B of the biuret group would lead to the formation of extended sheet-like structures, which may be unstable in solution and eventually lead to the formation of vesicle-like aggregates. The observed possible intermediate structures (Figure 1c, d) vividly implied that the formation of vesicles could be ascribed to pearling and budding mechanisms, which compete with each other and are not mutually exclusive. The formation of vesicle-like nanostructures in the THF solution is not limited to a specific case like molecule **2**, but also generally observed in other cases of linear π-conjugated cores doubly end-capped with the biuret group. Therefore, linear molecules, such as **4** and **5** that are capable of emitting green and orange-red fluorescence, respectively, can also generate vesicle-like nanospheres. Given that vesicle-like aggregates are relatively dispersed and highly luminescent, the emission spectra from each single nanovesicle can be collected using confocal fluorescence microscopy. The obtained spectra minimally varied between aggregates and were limitedly red-shifted as compared to those from the THF solution. Energy transfer processes are highly efficient in artificial vesicles because of fast exciton migration and proximity of the chromophores, which provides the opportunity to generate single aggregates whose emission colors can be tuned over a wide spectral range by simply adjusting the composition of the THF solutions from which aggregates are drop-cast. The vesicles obtained from a special case of THF solution composed of **2** (10^{-4}M), **4** (0.20 mol%), and **5** (0.25 mol%) gave a very clean white light emission corresponding precisely to the D65 standard when excited at 385 nm. The differences of colors from an area (10 × 10 μm) containing approximately 200 vesicles were minimal, indicating that the individual components are homogeneously dispersed within the vesicle and that the multiple energy transfer processes between identical (exciton hopping) and different chromophores were highly efficient.[2] The spontaneous formation of well-dispersed nanospheres in organic media is a fascinating phenomenon. Particularly, the nanovesicles self-assembled from the biuret-capped electroactive structures show high stability on a variety of substrates (SiO_2, Si, or ITO), thus making the system promising for future in-depth studies on the electronic properties of nanovesicles, and the possibility for inclusion of vesicles into organic electroluminescent devices.

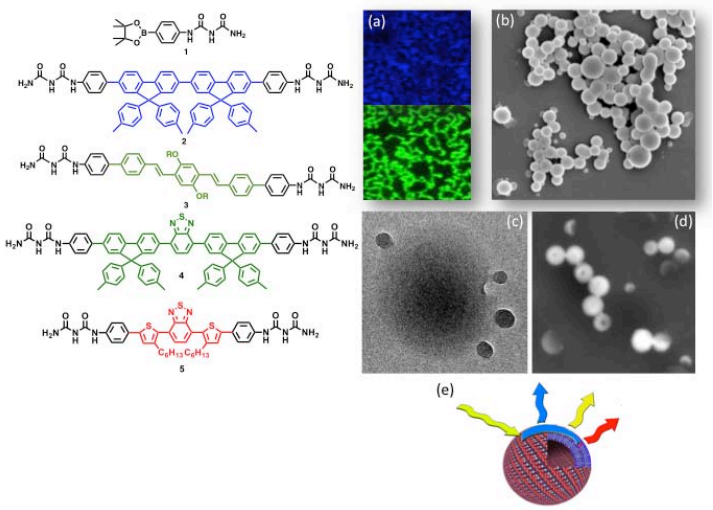

Figure 1. Chemical structures of biuret-containing molecules, and confocal fluorescence images of a film from a mixture of **2** and **3** (10%)(a), SEM image of the spherical nanaostructure from a THF solution of **2** (b), intermediate structures showing the budding mechanism (c) and pearling mechanism (d), white light-emitting vesicle of a mixture of molecules **2**, **4**, and **5**.

The morphology of self-assembled nanostructures is generally governed by the interplay of various intermolecular non-covalent interactions. Therefore, nano-morphology can be controlled and/or switched by manipulating the subtle balance between different non-covalent interactions. Along this line, a porphyrin derivative (**6**) incorporating orthogonally arranged octyl chains and H-B groups was developed to demonstrate the reversible transformation of aggregate morphology through exposure to different solvents. In polar protic (MeOH) environments, the H-B interactions between the biuret groups are disrupted, whereas the dominant van der Waals interaction between octyl chains lead to the formation of rod-like aggregates. The reverse occurs in polar aprotic media (THF), which favors H-B over hydrophobic interactions to induce the formation of spherical aggregates. Interestingly, the switch between rod and vesicle is entirely reversible and can take place as the nanostructures have been deposited on the substrate. In addition, supramolecular self-assembly capable of performing multiple responses toward the

outside stimuli can be achieved by the rational design of building blocks endowed with targeted functionality. For example, a linear compound (**7**) with a photoresponsive azobenzene core bearing with terminal phenylbiuret units and *n*-hexyl groups was recently prepared to demonstrate the feasibility of combining light-driven and solvent-drivenmorphological transformations. The morphology transitions have been observed in various solvent polarities. For example, in THF–hexane, the hydrophobic interactions of the alkoxyl chains are rather weak, producing amorphous networks. As hydrophilicity increases (THF/H_2O = 1/5), hydrophobic interactions are strengthened, leading to the formation of ordered sheets. As hydrophilicity is further increased (THF/H_2O = 1/20), the sheets are reorganized into spheres. The formation of fibrillar networks upon drop-casting from a THF solution of *trans*-**7** was observed similar to the case of molecule **3**.

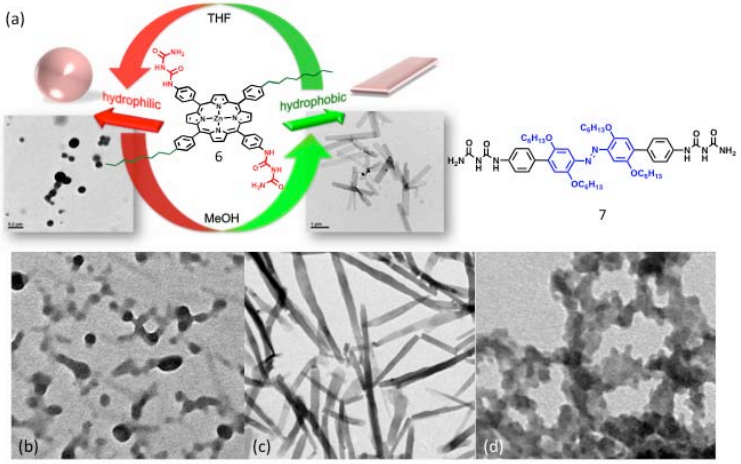

Figure 2. Reversible interconversion between nano-rods and hollow spheres self-assembled from molecule **6** upon exposure to different solvents (a), TEM images of nanostructures obtained form a solution of molecule **7** in THF/H_20 (1/5) (b), (1/20) (c) and (1/5) after irradiation with UV light (377 nm) (d).

The morphology is completely changed from fibers into hollow spheres after irradiating a *trans*-**7** solution with UV light (377 nm, 30

min). Interestingly, the progressive interconversion between the two morphologies can be identified with a short exposure time (15 min), where both fibrillar and spherical aggregates are present simultaneously. Although the photostationary state is composed of a majority of the *trans*-isomer, because of the cooperative effects of non-covalent interactions, the minority component (36% *cis*-isomer) is sufficient to drive the complete transition from fibers to spherical aggregates. More importantly, the photo-driven morphological transformations are reversible. Using a long-wavelength light (450 nm, 45 min) to irradiate a solution with spherical aggregates obtained from UV treatment led to the exclusive formation of fibrous aggregates.[5]

In summary, the rigid π-conjugated systems containing biuret as terminal H-B motifs are capable of self-assembling to give photoactive nanovesicles in organic media. The neutral, electro-active, and photoactive molecular structures make nanovesicles feasible for the realization of electroluminescence from a discrete nanostructure. The incorporation of alkyl groups perpendicularly grafted from the biuret-capped π-core enables the morphology of nanostructures to subtly adjust to the solvent polarity. Adjustment to solvent polarity is based on the interplay of H-B and hydrophobic interactions. Furthermore, a molecular system combining H-B, hydrophobic, and photoisomerizable motifs can smartly and reversibly response to both solvent polarity and light, thus demonstrating basic ideas for the design of adaptive materials.

References

1. Fang, F.-C.; Chu, C.-C.; Huang, C.-H.; Raffy, G.; Del Guerzo, A.; Wong, K.-T.; Bassani, D. M. *Chem. Commun.* 6369-6371, (2008).
2. Tseng, K.-P.; Fang, F.-C.; Shyue, J.-J.; Wong, K.-T.; Raffy, G.; Del Guerzo, A.; Bassani, D. M. *Angew. Chem. Int. Ed.* **50**, 7032-7036, (2011).
3. Velu, S. K. P.; Yan, M.; Tseng K.-P.; Wong, K.-T.; Bassani, D. M.; Terech, P. *Macromolecules*, **46**, 1591-1598, (2013).
4. Kuo, M.-C.; Chen, H.-F.; Shyue, J.-J.; Bassani, D. M.; Wong, K.-T. *Chem. Commun.* **48**, 8051-8053, (2012).

5. Tseng, K.-P.; Tsai, Y.-T.; Wu, C,-C; Shyue, J,-J; Bassani, D.M.; Wong, K,-T. *Chem. Commun*. **49**, 11536-11538, (2013).

Fluorescent organic nanocrystals as new imaging agents for confocal laser endomicroscopy

*Marine Soulié,[1] Abdelhamid Ghodbane,[1,2] Kacem Khemakhem,[1,2,3] Clara Fournier-Noël [1,2] and Suzanne Fery-Forgues [1,2]**

[1] CNRS & Université de Toulouse, ITAV-USR3505, 31106 Toulouse France; [2]CNRS & Université de Toulouse, IMRCP-UMR5623, 31062 Toulouse, France; [3]Laboratory of Applied Chemistry HCGP, Faculty of Science, University of Sfax, 3038 Sfax, Tunisia.

** suzanne.fery-forgues@itav.fr*

Gastrointestinal (GI) cancer is characterized by its aggressiveness. Colon cancer is currently the second leading cause of cancer death in Europe and, although less common, esophageal cancer is rarely curable. In this context, early diagnosis and treatment can markedly increase the life expectancy of patients. Confocal laser endomicroscopy (CLE) is a major technological advance for the early detection and ablation of dysplastic lesions or adenocarcinoma within GI tract.[1] It allows *in vivo* microscopy of the human GI mucosa during upper or lower endoscopy. Resolution is excellent. In contrast, distinguishing between normal and cancer cells is difficult. There is an urgent clinical need for increasing the detection sensitivity of this technique and this may depend on the development of new specific imaging agents. In this respect, injectable nanoparticles (NPs) were considered because they offer distinct advantages compared to dissolved dyes for *in vivo* applications. Owing to their size, they escape renal clearance, and surface chemistry allows their biological properties to be modified. The originality of our NPs is that their core is made of self-assembled fluorescent organic dyes.[2,3] Contrary to doped systems, these NPs are heavily loaded in dye molecules. They are intended to be very bright when adsorbed on the diseased tissues. Fluorescence must also be retained if NPs dissolve near their target, for example after internalization in cells. A key-step is thus the development of dyes that are strongly fluorescent both in the solid state and in solution. Dyes must also satisfy other criteria. In

particular, they must be excitable at the wavelengths delivered by medical lasers (488 and 660 nm) and have low toxicity.

Very few organic dyes are fluorescent in the solid state.[4] Their design means taking account both of their intrinsic emission properties and the molecular arrangement in the condensed state. In particular, the common π-π stacking of fluorophores is very detrimental to photoluminescence and must absolutely be avoided. A systematic work was undertaken on several families of neutral dyes (e.g. coumarins [5] and naphthoxazoles [6]) to optimize photoluminescence efficiency. Crystalline dyes were preferred because they offer precise control of the optical properties. Many of them showed photoluminescence quantum yields higher than 10%. Their solid-state emission covered much of the visible spectrum.

Alternatively, organic salts were investigated. They consist in a charged dye associated to a spectroscopically-silent organic counter-ion. The counter-ion plays a prominent role in the molecular arrangement and thus strongly influences the optical properties of the formed salt. Since counter-ions are easily interchangeable, the versatility of these systems reduces the effort in synthesis and enhances the potential of a dye for a given application. Extensive work was done with salts of berberine, a natural alkaloid known for its biological and photochemical activities.[7] Some of these salts were more emissive in the solid state than in solution and thus are an original example of crystallization-induced emission.[8]

Attention was then given to generating NPs from these dyes. Simple preparation methods, such as the reprecipitation method based on solvent exchange, were optimized to control the NP size and morphology. The effect of experimental parameters, in particular the presence of polymers used as additives, was thoroughly studied. In some cases, NPs below 80 nm were obtained.

In the frame of our EuroNanoMed "FONDIAG" project, the toxicity and incorporation mode of plain NPs were studied in collaboration with biologists (B. Ducommun, ITAV Toulouse). The NP surface was coated by modified polysaccharides to increase biocompatibility and affinity for cancer cells thanks to Warburg effect (T. Ciach, Warsaw University). Peptides selective for GI cancers were grafted to favour targeting (O. Marin, University of Padova) (Fig. 1). The first complete NPs are presently being tested on tumour-bearing rats by a team of gastro-enterologists (S. Realdon and G. Battaglia, IOV Padova). The first results are encouraging.

Projects are under way to enhance the selectivity of our NPs for use in diagnosis and personalized medicine. More broadly, our know-how in solid state emissive dyes can lead to unexpected applications both within the health field and in the field of fluorescent materials.

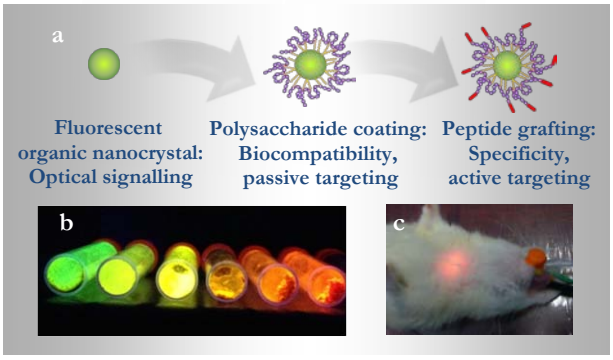

Figure 1. a) Concept of fluorescent organic NPs. b) Solid-state fluorescent coumarin derivatives. c) Exploration of rat esophagus by CLE.

References.

1. Goetz, M.; Kiesslich, R. *Anticancer Res.* **28**, 353-360 (2008).
2. Klymchenko, A. S. *J. Nanosci. Lett.* **3**:21 (2013).
3. Fery-Forgues, S. *Nanoscale*, **5, 8428-8442** (2013).
4. Cornil, J.; Beljonne, D.; Dos Santos, D. A.; Calbert, J. P.; Shuai, Z.; Brédas, J.-L. *C. R. Acad. Sci. Paris*, *Series IV*, 403-408 (2000).
5. Abid-Jarraya, N.; Turki-Guermazi, H.; Khemakhem, K.; Abid, S.; Saffon, N.; Fery-Forgues, S. *Dyes Pigm.* **101**, 164-171 (2014).
6. Ghodbane, A.; Colléaux, J.; Saffon, N.; Mahiou, R.; Galaup, J.-P.; Fery-Forgues, S. *ChemPlusChem* **78**, 185-191 (2013).
7. Chahine, J.; Saffon, N.; Cantuel, N. ; Fery-Forgues, S. *Langmuir* **27**, 2844-2853 (2011).
8. Fery-Forgues, S. Aggregation-induced emission in organic ion pairs. *In: Aggregation-Induced Emission: Fundamentals*, Tang B. Z.; Qin, A. (Eds), Singapore: John Wiley & Sons, Ltd., ISBN 978-1-118-39430-4, 104-124 (2014).

A Robust and Versatile Synthetic Route Towards PEGylated Luminescent Silica Nanoparticles

Enrico Rampazzo and Damiano Genovese
Department of Chemistry "G. Ciamician", University of Bologna, Italy

The incorporation of luminescent dyes in silica nanoparticles (NPs) is a powerful strategy to obtain labels[1,2] and sensors.[3] These systems can be achieved mainly by sol-gel processes using tetraethoxysilane (TEOS) as silica precursor, with synthetic strategies that share characteristics like simplicity, low costs, versatility and control over nanoparticle dimensions.

The most important synthetic approaches are the Stöber-Van Blaaderen method,[4,5] (with its heterogeneous mixtures,[6] and heterogeneous nucleation versions[15]) the reverse microemulsions (water-in-oil),[7] and the direct micelles assisted methods.[8-10] Each synthetic approach presents advantages and limitations that are transferred to the resulting nanostructures, designed to fit the desired application. Table 1 gives - for comparison purpose - a qualitative overview of the main aspects of the main strategies available for silica NPs synthesis.

As a general indication, the use of trialkoxysilane derivatized dyes,[11] ensures condensation of the fluorophores within the silica matrix, avoiding dye leaching in biological applications and in NPs having high surface-to-volume ratio. Some limitations to the doping process are mainly related to solubility and to the electrostatic interaction between the dye and silica, which in general favours the inclusion of positively charged dye, and hampers the one of negatively charged ones. In this short contribution we will focus on the direct micelles assisted methods using aggregates of high molecular weight surfactants as templates.

The lipophilic nature of silica precursors such as TEOS or other organo-alkoxysilane and of most of the organic dyes allow the use of micellar aggregates or co-aggregates in water as self-organized templates to confine the silica nanoparticles growth. Within this general strategy, a main distinction can be made referring to the molecular weight of the surfactant that is used.

Table 1: Schematic comparison of NPs synthetic methods: approx. size range in the case of one-pot synthesis and other main features (+ adequate; ++ good: +++ excellent).

	Dimensional Range (nm)	Tuning of NPs diameter	Pristine Colloidal Stability	Dyes Incorporation	Surface Modification	Accessibility to core-shell and hybrid architectures
Stöber-Van Blaaderen	~ 10-800	+++	+++	++	+	+
Stöber-biphasic	~ 5-500	+++	+++	+	+	++
Wiesner C-Dots	~ 5-100	++	+++	+++	++	+
Reverse microemulsion (Water-in-Oil)	~ 15-200	+++	++	+	+++	+++
Direct Micelles (ORMOSIL)	~ 10-250	++	++	++	+++	++
Direct Micelles (Pluronic F127)	~ 10-100	+	+++	+++	+++	++

Using low molecular weight surfactants such as AOT (Bis(2-ethylhexyl) sulfosuccinate sodium salt) or Tween 80, Prasad and coworkers gave the largest part of the contributions in the field: the ORMOSIL (ORganic - MOdified – SILica) systems they developed, exploited the hydrolysis of lipophilic silica precursor such as VTES (triethoxyvinylsilane) in the presence of APTES (3-aminopropyltriethoxysilane) or ammonia. These NPs, had a diameter spanning in the 20-30 nm, with a mesoporous silica matrix were suitable for PDT applications,[12] with dyes that usually need to be covalently linked to the nanoparticle to avoid leaching.[13,14] Functionalization with groups such as -NH_2, -COOH, -SH conferred targeting and labelling capabilities for conjugation with bioactive molecules.[15] Similar synthetic strategies were used to obtain PEGylated NPs,[16] or for the incorporation of QDs[17] and Fe_3O_4 nanoparticles.[18]

Other contribution in the field is the work of Wiesner and coworkers that developed tiny mesoporous PEGylated NPs (6-15 nm) in the presence of hexadecyltrimethylammonium bromide (CTAB) micelles. Interestingly, this strategy also affects the nanoparticle morphology,

which was found to depend by the average number of micellar aggregates entrapped in each nanoparticle core during the condensation process.[19]

A different synthetic possibility is to use a direct micelle assisted strategy with high molecular weight surfactants, such as Pluronic F127, F108, or Brij700 to synthesize cross-linked micellar NPs featuring core-shell structures,[8,20] size-tunable properties,[21] or bridging organo-silane precursors.[22] In most cases, these synthetic protocols are quite different from the Stöber approach, since the condensation processes are promoted in acidic environment, with acids such as HCl[22] or HOAc,[23] a set of conditions (pH < 4) in which the hydrolysis has faster kinetics with respect to the condensation rate and that stimulates the formation of Si-O-Si chains in the early stages of the polymerization,[24] that finally undergo cross-linking.[25] This promotes the confinement of the silica matrix in the micellar environment, and the entrapment-adsorption of these surfactants to the silica core, with the valuable consequence of nanoparticle surface modification in a single procedure.

Pluronic F127 (MW 12.6 KDa, Fig. 1), is up to now probably the most versatile surfactant for this kind of applications: a leading part in the development of fluorescent NPs obtained by Pluronic F127 micelles assisted method was played by our group (PluS NPs, Pluronic Silica NanoParticles).[1,26] Pluronic F127 is characterized by a tri-block PEG-PPO-PEG (poly(ethyle glycol)-poly(propylene oxide)-poly(ethylene glycol)) structure and quite large micellar aggregates in water (~ 22-25 nm). The PPO inner core of these aggregates enables to use TEOS as silica precursor instead of lipophilic organo-alkoxysilanes, contributing to a more stable and dense silica network, in which many kinds of alkoxysilane derivatized dyes, from polar to very lipophilic, can be condensed. This PEGylated core-shell NPs are very monodisperse and stable in water and physiological conditions. The versatility of these systems was exploited in several fields spanning from photophysical studies,[26,27] sensors,[3,28] biological imaging,[23] fluorescent-photoswitchable nanoparticles,[29] self-quenching recovery,[30] and ECL.[8,31] The core-shell structure (hard diameter 10 nm, hydrodynamic diameter 25 nm) was verified by several experimental techniques, such as TEM and DLS (Dynamic Light Scattering),[27] and AFM measurements.[8] ^{1}H-NMR showed the outward orientation of the shell PEG chains, while TGA (Thermo Gravimetric Analysis) performed on samples subjected to

ultrafiltration verified the irreversible linking between surfactant and silica core.[31]

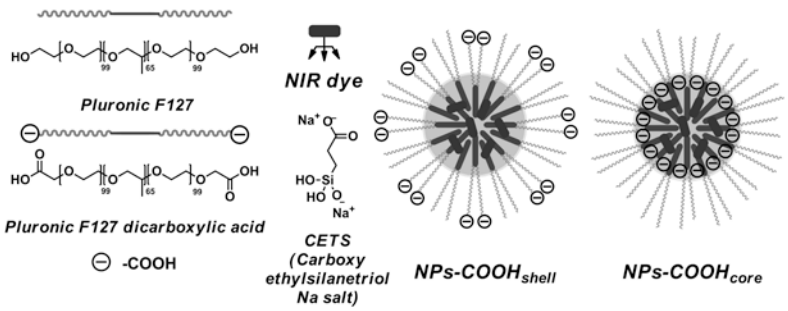

Figure 1. NIR fluorescent PluS NPs for *in vivo* limph node mapping, by different positioning schemes of negative groups (-COO^-).

The functionalization of these nanostructures was achieved modifing the Pluronic F127 hydroxy end groups, for labelling[32] or non-specific targeting.[33] We found that cellular uptake was influenced by nanoparticle functionalization, and PluS NPs cytotoxicity was negligible for nanoparticles with an external PEG shell or presenting external amino- or carboxy-groups toward several normal or cancer cell types, grown either in suspension or in adherence.[33]
Recently we exploited the core-shell nature of these NPs to develop NIR fluorescent NPs for regional lymph nodes mapping (Fig. 1).[34] We synthesized negatively charged NPs having programmed charges positioning schemes to influence their biodistribution for lymph nodes targeting *in vivo*. We found that NPs having negative charges in the mesoporous silica core – hidden by a PEG shell - demonstrated a more efficient and dynamic behaviour during lymph nodes mapping. This last example showed once again the versatility of the core-shell silica-PEG structure, were the modifications of both core and shell parts play a synergistic effect in defining the efficiency of the fluorescent probe.

References.

1. Bonacchi, S.; Genovese, D.; Juris, R.; Montalti, M.; Prodi, L.; Rampazzo, E.; Zaccheroni, N. *Angew. Chem. Int. Ed.*, **50**, 4056-4066 (2011).
2. Montalti, M.; Prodi, L.; Rampazzo, E.; Zaccheroni, N. *Chem. Soc. Rev.*, 10.1039/c1033cs60433k (2014).
3. Montalti, M.; Rampazzo, E.; Zaccheroni, N.; Prodi, L. *New J. Chem.*, **37**, 28-34 (2013).
4. Stöber, W.; Fink, A.; Bohn, E. *J. Colloid Interface Sci.*, **26**, 62-69 (1968).
5. Van Blaaderen, A.; Vrij, A. *Langmuir*, **8**, 2921-2931 (1992).
6. Wang, J.; Sugawara-Narutaki, A.; Fukao, M.; Yokoi, T.; Shimojima, A.; Okubo, T. *ACS Appl. Mater. Inter.*, **3**, 1538-1544 (2011).
7. Bagwe, R. P.; Hilliard, L. R.; Tan, W. *Langmuir*, **22**, 4357-4362 (2006).
8. Zanarini, S.; Rampazzo, E.; Bonacchi, S.; Juris, R.; Marcaccio, M.; Montalti, M.; Paolucci, F.; Prodi, L. *J. Am. Chem. Soc.*, **131**, 14208-14209 (2009).
9. Yong, K. T.; Roy, I.; Swihart, M. T.; Prasad, P. N. *J. Mater. Chem.*, **19**, 4655-4672 (2009).
10. Bagwe, R. P.; Yang, C.; Hilliard, L. R.; Tan, W. *Langmuir*, **20**, 8336-8342 (2004).
11. Verhaegh, N. A. M.; Blaaderen, A. v. *Langmuir*, **10**, 1427-1438 (1994).
12. Kim, S.; Ohulchanskyy, T. Y.; Pudavar, H. E.; Pandey, R. K.; Prasad, P. N. *J. Am. Chem. Soc.*, **129**, 2669-2675 (2007).
13. Kim, S.; Huang, H.; Pudavar, H. E.; Cui, Y.; Prasad, P. N. *Chem. Mater.*, **19**, 5650-5656 (2007).
14. Selvestrel, F.; Moret, F.; Segat, D.; Woodhams, J. H.; Fracasso, G.; Echevarria, I. M. R.; Bau, L.; Rastrelli, F.; Compagnin, C.; Reddi, E. *et al. Nanoscale*, **5**, 6106-6116 (2013).
15. Kumar, R.; Roy, I.; Ohulchanskyy, T. Y.; Goswami, L. N.; Bonoiu, A. C.; Bergey, E. J.; Tramposch, K. M.; Maitra, A.; Prasad, P. N. *ACS Nano*, **2**, 449-456 (2008).
16. Kumar, R.; Roy, I.; Ohulchanskky, T. Y.; Vathy, L. A.; Bergey, E. J.; Sajjad, M.; Prasad, P. N. *ACS Nano*, **4**, 699-708 (2010).
17. Seddon, A.; Li Ou, D. *J. Sol-Gel Sci. Technol.*, **13**, 623-628 (1998).
18. Law, W.-C.; Yong, K.-T.; Roy, I.; Xu, G.; Ding, H.; Bergey, E. J.; Zeng, H.; Prasad, P. N. *J. Phys. Chem. C*, **112**, 7972-7977 (2008).

19. Ma, K.; Werner-Zwanziger, U.; Zwanziger, J.; Wiesner, U. *Chem. Mater.*, **25**, 677-691 (2013).
20. Chi, F.; Guan, B.; Yang, B.; Liu, Y.; Huo, Q. *Langmuir*, **26**, 11421-11426 (2010).
21. Chi, F.; Guo, Y.-N.; Liu, J.; Liu, Y.; Huo, Q. *J. Phys. Chem. C*, **114**, 2519-2523 (2010).
22. Liu, J.; Bai, S.; Zhong, H.; Li, C.; Yang, Q. *J. Phys. Chem. C*, **114**, 953-961 (2009).
23. Rampazzo, E.; Boschi, F.; Bonacchi, S.; Juris, R.; Montalti, M.; Zaccheroni, N.; Prodi, L.; Calderan, L.; Rossi, B.; Becchi, S. *et al. Nanoscale*, **4**, 824-830 (2012).
24. Cushing, B. L.; Kolesnichenko, V. L.; O'Connor, C. J. *Chem. Rev.*, **104**, 3893-3946 (2004).
25. Gallagher, D.; Ring, T. A. *Chimia*, **43**, 298 (1989).
26. Pedone, A.; Gambuzzi, E.; Barone, V.; Bonacchi, S.; Genovese, D.; Rampazzo, E.; Prodi, L.; Montalti, M. *PCCP*, **15**, 12360-12372 (2013).
27. Rampazzo, E.; Bonacchi, S.; Juris, R.; Montalti, M.; Genovese, D.; Zaccheroni, N.; Prodi, L.; Rambaldi, D. C.; Zattoni, A.; Reschiglian, P. *J. Phys. Chem. B*, **114**, 14605-14613 (2010).
28. Rampazzo, E.; Bonacchi, S.; Genovese, D.; Juris, R.; Sgarzi, M.; Montalti, M.; Prodi, L.; Zaccheroni, N.; Tomaselli, G.; Gentile, S. *et al. Chemistry – A European Journal*, **17**, 13429-13432 (2011).
29. Genovese, D.; Montalti, M.; Prodi, L.; Rampazzo, E.; Zaccheroni, N.; Tosic, O.; Altenhoner, K.; May, F.; Mattay, J. *Chem. Commun.*, **47**, 10975-10977 (2011).
30. Genovese, D.; Bonacchi, S.; Juris, R.; Montalti, M.; Prodi, L.; Rampazzo, E.; Zaccheroni, N. *Angew. Chem. Int. Ed.*, **52**, 5965-5968 (2013).
31. Valenti, G.; Rampazzo, E.; Bonacchi, S.; Khajvand, T.; Juris, R.; Montalti, M.; Marcaccio, M.; Paolucci, F.; Prodi, L. *Chem. Commun.*, **48**, 4187-4189 (2012).
32. Soster, M.; Juris, R.; Bonacchi, S.; Genovese, D.; Montalti, M.; Rampazzo, E.; Zaccheroni, N.; Garagnani, P.; Bussolino, F.; Prodi, L. *et al. Int. J. Nanomed.*, **7**, 4797-4807 (2012).
33. Rampazzo, E.; Voltan, R.; Petrizza, L.; Zaccheroni, N.; Prodi, L.; Casciano, F.; Zauli, G.; Secchiero, P. *Nanoscale*, **5**, 7897-7905 (2013).
34. Helle, M.; Rampazzo, E.; Monchanin, M.; Marchal, F.; Guillemin, F.; Bonacchi, S.; Salis, F.; Prodi, L.; Bezdetnaya, L. *ACS Nano*, **7**, 8645-8657 (2013).

PILLS OF HISTORY

At the origin of photochemistry. The photochemical behavior of santonin. Some considerations on the published documents.

Maurizio D'Auria
Dipartimento di Scienze, Università della Basilicata, Viale dell'Ateneo Lucano 10, Potenza, Italy

In the previous issue of the *EPA Newsletter* we reported some document related to the history of the study on the photochemical behavior of Santonin. Here we want to report some considerations on the same argument on the basis of the reported documents. Santonin is an anthelminthic compound isolated in *Artemisia maritime* and *Artemisia cina* (Compositae) (Figure 1).

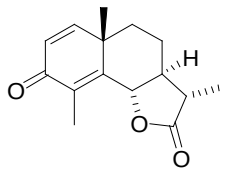

Figure 1. Santonin

The first report on the photochemical behavior of santonin is the observation of the apothecary Kahler. He obtained santonin from *Artemisia* and noted that in the presence of sunlight the substance became yellow.[1]
Some years later, Trommsdorff confirmed that santonin, under the effect of sunlight, became yellow.[2] Heldt in 1847 showed that, under irradiation, santonin crystals became yellow and that santonin "crystals are cleaved first along cuts normal to the long axis; the inclined crystal faces are also separated along cuts perpendicular to the long axis. The newly created surfaces are not planar but have quite irregular boundaries. If A is the top view of the crystal, the lines a, b, c indicate the direction of cleavage" (Figure 2).[3,4]

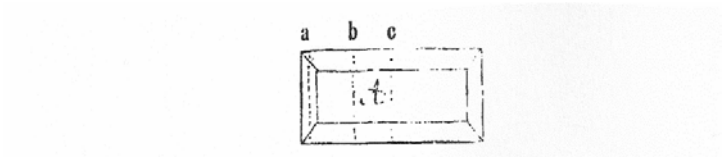

Figure 2. The cuts on the crystals of santonin when it was irradiated in the presence of sunlight.

Yellow santonin has been studied by Montemartini.[5] He did not confirm the observations of Heldt; he did not find differences in uncolored and colored crystals, and he found the same cleavage fractures. He found that the melting point of santonin decreased, also the α_D of santonin decreased. However, the composition of the yellow product was the same of that of santonin. Crystallization of yellow santonin gave uncolored crystals of santonin. However, yellow santonin reacted with $KMnO_4$ while santonin was resistant to the oxidation. The main product obtained in the reaction of santonin with $KMnO_4$ was ossalic acid, while yellow santonin did not give this compound. Montemartini concluded his work considering that yellow santonin could differ from santonin for the distribution of the bonds in the hydronaphthyl scaffold of santonin.

Sestini, some year after the work of Heldt, found a new photochemical reaction. Irradiating with solar light an alcoholic solution of santonin, he found that the addition of a large volume of water allowed the precipitation of an uncolored substance and he named it photosantonin.[6] After more than ten years he described an improved method to obtain photosantonin when the reaction is conducted in acetic acid.[7] In this case, the photosantonic acid was obtained. The procedure was implemented by Villavecchia: "A solution of santonin in alcohol (90 °) obtained dissolving 20 g. of santonin every liter of alcohol was irradiated with sunlight for 3 months. The yellow liquid was distilled under vacuum to eliminate the solvent; to the residue (a dense oil colored in yellow-brown) a warm solution of sodium carbonate was added. The solution was gentle warmed. The product dissolved in the alcoholic solution was obtained after saturation with hydrochloric acid, and gave crystals of photosantonic acid. The fraction insoluble in sodium carbonate was dissolved in ether and from this solution tubular crystals were obtained with m.p. 154-155 ° (...). Slow evaporation of the ethereal solution gave crystals with m.p. 68-69 °, identical to photosantonin of

Sestini".[8,9] This procedure was followed by Francesconi and Maggi when they studied the synthesis of some derivatives of photosantonin.[10]

In the same period Cannizzaro studied the photochemical behavior of santonin. The reaction was performed in acetic acid. The evaporation of the solvent allowed to isolate photosantonic acid on the filter while the liquid phase contained a new product of the reaction, named isophotosantonic acid.[11,12] Is it the same type of compounds isolated by Villavecchia when the reaction was performed in ethanol? I think so considering that, as the compound isolated by Villavecchia, it showed a positive value of α_D, while photosantonin showed a negative value of this parameter. In that paper Cannizzaro proposed a structure for santonin (Fig. 3). This structure is not similar to the actual one.

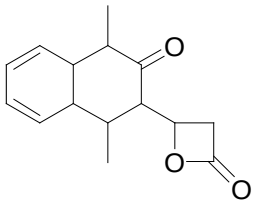

Figure 3. The first structure proposed by Cannizzaro for Santonin.

On the basis of this structure Cannizzaro proposed a structure for photosantonic acid and isophotosantonic acid (Fig. 4).

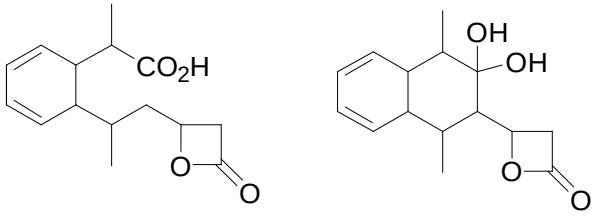

Figure 4. Structures proposed by Cannizzaro for photosantonic acid (left) and isophotosantonic acid (right).

These unrealistic structures were corrected some years later. In 1893 Cannizzaro, on the basis of his previous work[13] and that of Gucci

and Grassi Cristaldi,[14] gave its structure of santonin, a structure not so different as that accepted now, and that of photosantonin (Fig. 5).[15]

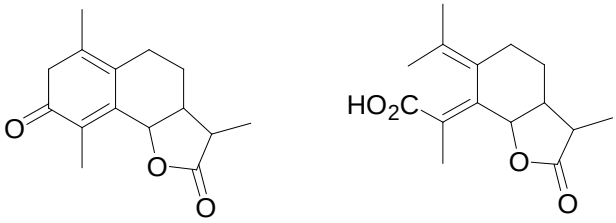

Figure 5. Santonin (left) and photosantonin (right) structure proposed by Cannizzaro.

We have to wait for a long time in order to solve the question. The structure of photosantonic acid has been established in 1958 by van Tamelen.[16,17] Furthermore, the mechanism of the photoisomerization was clarified only in 1963 through the isolation and identification of all the intermediates of the reaction (Scheme 1).[18-20]

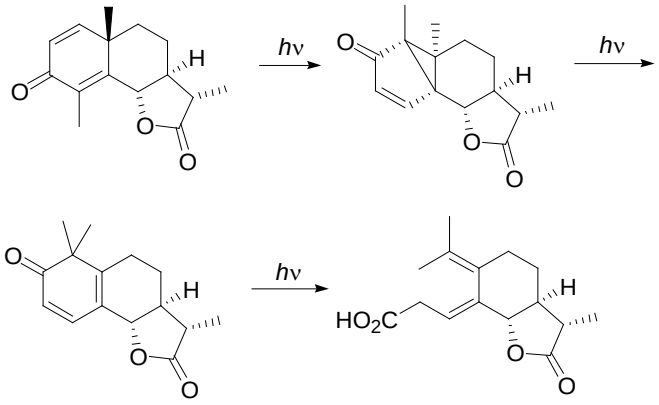

Scheme 1. The photoisomerization of Santonin

References

1. Kahler *Arkiv der Pharmazie* **34**, 318-319 (1830).
2. Trommsdorff, H. *Annalen der Pharmacie* **11**, 190-208 (1834).

3. Heldt, W. *Justus Liebigs Annalen der Chemie* **63**, 10-83 (1847).
4. The translation is due to Roth, H. D. *Photochemical & Photobiological Sciences* **10**, 1849-1853 (2011).
5. Montemartini, C. *Gazzetta Chimica Italiana* **32**(I), 325-366 (1902).
6. Sestini, F. Fatti relativi alle metamorfosi chimiche della santonina. *Repertorio Italiano di Chimica e Farmacia*, Firenze, 1865.
7. Sestini, F. *Gazzetta Chimica Italiana* **6**, 357-369 (1876).
8. Villavecchia, V. *Berichte der deutschen chemischen Gesellschaft* **18**, 2859-2864 (1885).
9. Villavecchia, V. *R. Acc. Lincei, Rendiconti, series 4,* **1**, 721-726 (1885).
10. Francesconi, L. & Maggi, G. *Gazzetta Chimica Italiana* **33**(II), 65-78 (1903).
11. Cannizzaro, S. & Fabris, G. *Berichte der deutschen chemischen Gesellschaft* **19**, 2260-2265 (1886).
12. Cannizzaro, S. & Fabris, G. *R. Acc. Lincei, Rendiconti, series 4,* **2**, 448-453 (1886).
13. Cannizzaro, S. *Gazzetta Chimica Italiana* **13**, 385 (1883).
14. Gucci, P. & Grassi-Cristaldi, G. *Gazzetta Chimica Italiana* **22**(I), 1-55 (1892).
15. Cannizzaro, S. & Gucci, P. *Gazzetta Chimica Italiana* **23**(I), 286-294 (1893).
16. van Tamelen, E. E., Levin, S. H., Brenner, G. Wolinsky, J. & Aldrich, P. *Journal of the American Chemical Society* **80**, 501-502 (1958)
17. van Tamelen, E. E., Levin, S. H., Brenner, G., Wolinsky, J. & Aldrich, P. *Journal of the American Chemical Society* **81**, 1666-1678 (1959).
18. Barton, D. H. R., De Mayo, P. & Shafiq, M. *Proceedings of the Chemical Society*, 205 (1957).
19. Chapman, O. L. & Englert, L. F. *Jouranl of the American Chemical Society* **85**, 3028-3029 (1963).
20. Fisch, M. H. & Richards, J. H. *Journal of the American Chemical Society* **85**, 3029-3030 (1963).

ABSTRACTS OF THESIS IN PHOTOCHEMISTRY

Oligothiophenes Synthesis and High-Resolution Spectroscopic Characterization

Ambra Guarnaccio
Department of Science, Università della Basilicata, Viale dell'Ateneo Lucano 10, 85100 Potenza, Italy
Ph.D. Thesis (in English), 2013; Research Adviser: Maurizio D'Auria, Roberto Teghil, Antonio Santagata

1. Motivation and aim of this work

Recently, developing inexpensive renewable energy sources has stimulated tremendous interest in construction of light energy conversion systems.[1] For these purposes, covalent oligomer-fullerene donor-acceptor structures can be used as an important model systems for 'plastic' photovoltaic (PV) cells based on interpenetrating networks of conjugated polymers and fullerene derivatives.
Among the most popular and satisfactory photovoltaic materials oligothiophenes are widely envisaged as components of artificial molecular devices to mimic light energy conversion. In this work, conjugated oligothiophene oligomers have been chosen as model compounds for photovoltaic applications. Some oligomers have been synthesized, functionalized and, finally, coupled to fullerene C_{60} in such a way that a well-defined donor-acceptor triad molecule has been obtained and studied as individual molecule in both solution and solid state.
The first step of our efforts has been directed to setup a synthetic pathway towards new oligothiophenes materials with intermediate functions. First of all, performing well known oligothiophenes synthesis has provided the starting monomeric material reported in the following Figure 1:

Figure 1. 1,3-di(thiophen-2-yl)benzo[c]thiophene.

Figure 2. 1,3-Bis(5-ethynyl-2-thienyl)benzo[c]thiophene-di(hydrofullerene).

After the synthesis of this target compound our aim has been to develop further the synthesis of new oligothiophenes analogues with extended conjugation and, as a direct consequence, lower energy gap (lower HOMO-LUMO gap). Every synthetic step has been conducted with the objective of developing a suitable low consumption of the starting materials and time saving approaches.
After the initial production of monomers we designed new synthetic pathways aiming to produce new donor-acceptor systems potentially useful for photovoltaic applications. The basic idea is to incorporate a fullerene cage into the designed molecular triads which offers an optimal balance between synthetic accessibility, processability, and efficient photoresponsibility as expected for applications in photovoltaic devices. To date, many electro- and photo-active

chromophores have been incorporated in donor-acceptor molecular arrays on the basis of fullerene derivatives.[2]

In particular, we have studied fullerene-linked oligothiophenes, in which the fullerene C_{60} is covalently bonded to the terminal position of oligothiophenes by two ethynyl bridges.[3] With this aim the scaffold consisting of a new isothianaphthene-fullerene C_{60}-DTBT-C_{60} triad system has been prepared (see Figure 2).

It has been demonstrated that the concept of a linear arrangement of π-donor and π-acceptor can be extended to a triad system where the donor is integrated between two terminal acceptor units.[3] In oligothiophenes/fullerene dyad or triad systems, the fullerene behaves as an effective acceptor for intramolecular electron or energy transfer.[4] Photoinduced electron transfer is a key function for the construction of optoelectronic devices or artificial photosynthetic systems.[5]

2. Results and conclusions

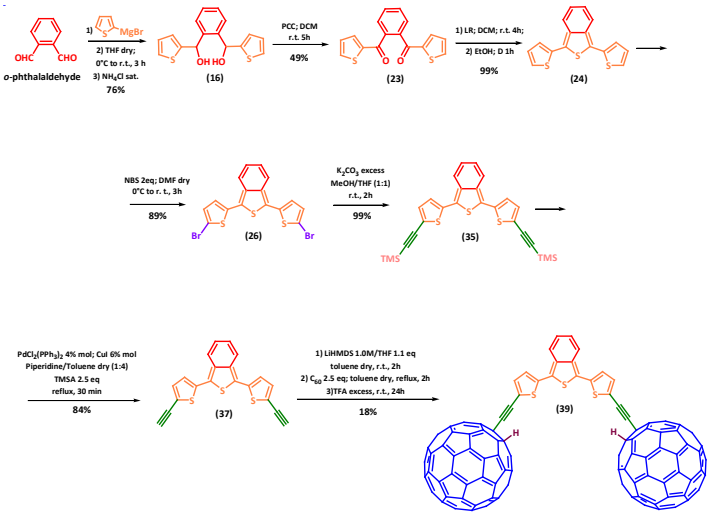

Scheme 1

Our initial aim to synthesize a promising oligothienylic candidate in order to study and develop a new material potentially useful for

organic photovoltaic applications has been reached. For this reason, the oligothienylic electron-donor DTBT compound (**24**) has been coupled with an electron acceptor counterpart (fullerene C_{60}) linked by two ethynyl bridges to have our new donor-acceptor compound (**39**).

The complete synthetic path of this new compound has been published on *Synlett* **2013**, *24*(8), 943-946 (DOI: 10.1055/s-0032-1316902). The synthetic pathway adopted is composed of seven consecutive steps starting from a commercially available and low cost ortho-phthalaldehyde (Scheme 1 below). The followed synthetic approach has allowed us to obtain a donor-acceptor target compound with a total yield around 26% after the first six reaction steps that drops to around 5% after the last critical reaction for fullerene coupling.

Starting from this result so far achieved, in the near future we will look forward to implement strategies aimed at improving the performance of the whole process but particularly that on the last step, the coupling of the fullerene ethynyl bridges which proved to be the critical step of the whole process. The idea is to change some parameter related to synthetic conditions in order to achieve the previously described objective with yield improvements.

After the synthesis two main strategies have been followed in order to verify the potential technological future applications of this new material. The first one with the aim to verify if an ultrafast electron transfer process could happen between the two dissimilar counterparts. These studies have been performed by Pump-Probe measurements that allowed us to show the evidence of an electron transfer process occurring in the donor-acceptor system.

Concerning the first strategy adopted, the photophysical characterization of the synthesized donor-acceptor system has been then accomplished. The characterization of the ground state has been processed through steady-state techniques like UV-vis absorption and emission spectra. From these two measurements it has been concluded that the system under analysis shows a pronounced coupling of donor and acceptor counterparts in the ground state. Moreover, if we compare emission spectra related to donor alone and donor-acceptor system, an important quenching of fluorescence can be detected in polar solvents.

The evaluation about the possible ability of the synthesized donor-acceptor system to undergo a charge transfer from donor moiety

towards the acceptor counterpart has been performed with a preliminary theoretical DFT calculation. This has shown how the electron density is present, in the HOMO, over the oligothiophene donor part of the molecule while, in the LUMO the electron density is completely concentrated over the fullerene counterpart. In fact, our preliminary calculations (DFT/B3LYP/6-31G+(d,p)) show that the HOMO → LUMO transition could experience an electron-transfer process the HOMO is found at –0.17177 H and it is mainly localized on the DTBT part of the molecule; while the LUMO is found at 0.11032 H and localized on the fullerene.

Afterwards, time-resolved Pump-Probe measurements have been provided in order to study the electronic structure of the donor-acceptor system. About this matter we have been able to attribute some excited electronic states related to the system created after photoexcitation. The relative associated relaxation times and constants rates have been evaluated thanks to the kinetic analysis obtained from the Pump-Probe spectroscopic data. In the same time, a proof of an intramolecular indirect electron transfer process has been detected.

Since just some preliminary results have been collected, it would be needed in future, to perform other experimental evaluations about the parameters affecting the occurrence of this electron transfer phenomena. Anyway to the best of our knowledge it can be concluded that the donor-acceptor molecule designed and synthesized in this thesis could be a good candidate for organic solar cell applications with respect of the results shown in this thesis.

References

1. (a) Hagfeldt, A.; Gratzel, M. *Chem. Rev.* **1995**, *95*, 49-68. (b) Bonhote, P.; Moser, J.-E.; Humphry-Baker, R.; Vlachopoulos, N.; Zakeeruddin, S. M.; Walder, L.; Gratzel, M. *J. Am. Chem. Soc.* **1999**, *121*, 1324-1336. (c) Hagfeldt, A.; Gratzel, M. *Acc. Chem. Res.* **2000**, *33*, 269-277. (d) O'Regan, B.; Gratzel, M. *Nature* **1991**, *353*, 737-740. (e) Bach, U.; Lupo, D.; Comte, P.; Moser, J. E.; Weissortel, F.; Salbeck, J.; Spreitzer, H.; Gratzel, M. *Nature* **1998**, *395*, 583-585. (f) Cinnsealach, R.; Boschloo, G.; Rao, S. N.; Fitzmaurice, D. *Sol. Energy Mater. Sol. Cells* **1999**, *55*, 215-223. (g) Shah, A.; Torres, P.; Tscharner, R.; Wyrsch, N.; Keppner, H. *Science* **1999**, *285*, 692-698. (h)

Granstrom, M.; Petrisch, K.; Arias, A. C.; Lux, A.; Andersson, M. R.; Friend, R. H. *Nature* **1998**, *395*, 257-260. (i) Halls, J. J. M.; Walsh, C. A.; Greenham, N. C.; Marseglia, E. A.; Friend, R. H.; Moratti, S. C.; Holmes, A. B. *Nature* **1995**, *376*, 498-500.
2. (a) Martín, N.; Sánchez, L.; Illescas, B.; Pérez, I. *Chem. Rev.* **1998**, *98*, 2527-2548. (b) Imahori, H.; Sakata, Y. *Eur. J. Org. Chem.* **1999**, 2445-2457. (c) Guldi, D. M. *Chem. Commun.* **2000**, 321-327. (d) Gust, D.; Moore, T. A.; Moore, A. L. *Acc. Chem. Res.* **2001**, *34*, 40-48. (e) Guldi, D. M.; Kamat, P. V. In Fullerenes: Chemistry, Physics, and Technology; Kadish, K. M., Ruoff, R. S., Eds.; John Wiley and Sons: New York, 2000; Chapter 5, pp 225-281 and references therein.
3. (a) C. Ego, D. Marsitzky, S. Becker, J. Zhang, A. C. Grimsdale, K. Müllen, J. D. MacKenzie, C. Silva, R. H. Friend, *J. Am. Chem. Soc.* **2003**, *125*, 437–443; (b) F. Jäcke, S. De Fryter, J. Hofkens, F. Köhn, F. C. De Schryver, C. Ego, A. C. Grimsdale, K. Müllen, *Chem. Phys. Lett.* **2002**, *362*, 534–540; (c) L. M. Herz, C. Silva, R. H. Friend, R. T. Philips, S. Setayesh, S. Becker, D. Marsitsky, K. Müllen, *Phys. Rev. B* **2001**, 64, 195–203; (d) D. Beljonne, G. Pourtois, C. Silva, H. Hennebicq, L. M. Herz, R. H. Friend, G. D. Scholes, S. Setayesh, K. Müllen, J. L. Brédas, *Proc. Natl. Acad. Sci.* **2002**, *99*, 10982–10987.
5. For recent reviews on photo- or electro-active organofullerenes, see: (a) N. Martín, L. Sánchez, B. Illescas and I. Pérez, *Chem. Rev.,* **1998**, *98*, 2527; (b) M. Prato and M. Maggini, *Acc. Chem. Res.*, **1998**, *31*, 519; (c) D. M. Guldi, M. Maggini, N. Martin and M. Prato, *Carbon*, **2000**, *38*, 1615; (d) J. L. Segura and N. Martín, Chem. Soc. Rev., **2000**, *29*, 13; (e) D.M. Guldi and M. Prato, *Acc. Chem. Res.*, **2000**, *33*, 695.
5. For recent reviews on photoinduced electron and energy transfer, see: (a) D. Gust, T. A. Moore and A. L. Moore, *Acc. Chem. Res.*, **1993**, *26*, 198; (b) D. Gust, T. A. Moore and A. L. Moore, *Acc. Chem. Res.*, **2001**, *34*, 40; (c) D. Holten, D. F. Bocian and J. S. Lindsey, *Acc. Chem. Res.*, **2002**, *35*, 57.

Medium effect on photophysical properties of some organic compounds interesting in photovoltaic or non-linear optics applications.

Rebecca Flamini
University of Perugia, Department of Physics and Geology, via A. Pascoli, 06123 Perugia (Italy)
Ph.D. Thesis (in English), 2013; Research Adviser: Anna Spalletti

My thesis was nominated for the 2014 EPA Prize for the best PhD thesis in photochemistry. The thesis work aimed to investigate some symmetrically and asymmetrically substituted fluorene- and anthracene-based arylacetylenes for their potential use in organic photovoltaics (OPV) and non-linear optics (NLO). The research was addressed to these extended π-conjugated compounds because of their potential interest as active materials in light-emitting diodes, solar cells and field-effect transistor, also considering their great versatility and cost-effectiveness compared to the inorganic counterparts. Moreover, arylacetylenes are expected to have large two-photon cross section making them useful to collect both UV-Vis (one-photon absorption) and IR (two-photon absorption, TPA) radiation extending their absorption spectrum and enhancing the overlap with the solar emission spectrum, such as a true up-conversion.
The studied systems are generally characterized by intense absorption and emission bands which make them potentially useful also as fluorescence probes and solar absorbers in photovoltaic devices. The choice of compounds containing triple bonds as conjugation bridges assured a convenient thermal and photochemical stability, as well as good semiconductor properties.
The photophysical study, carried out using stationary and time-resolved spectrometric techniques, in solution and in the solid state as thin-films, enabled a detailed exploration of molecular architecture-electronic structure relationships of the components of bulk heterojunction (BHJ) OPV cells.
The thin-film absorption was found to cover a larger spectral region

if compared with that in the solution. The presence of both H- and J-aggregates was evidenced by the characteristic absorption features accompanied by bands due to residual "unstacked" species. Films of these arylacetylenes inside a fullerene acceptor (PCBM) matrix were also investigated. Indeed, interesting information useful to drive the design/synthesis towards more efficient charge-donor compounds came from the comparison between fluorescence quenching of the asymmetric and symmetric compounds in the PCBM blended films. For instance, the emission quenching observed for symmetric ones was particularly efficient, confirming the trend of the previously reported photovoltaic cell responses (up to 3%), whereas it was nearly absent for the *push-pull* systems bearing the cyano-group. Nevertheless, the introduction of electron-withdrawing peripheral groups in the anthracene-based donors caused red shifts of the absorption spectrum, leading to a better harvesting of the solar emission light.

Energy transfer processes from the absorbing "unstacked" species and H-aggregates to J-aggregates were observed, evidenced by prompt and delayed fluorescence and confirmed by ultrafast measurements.

In this work we also faced an approach aimed to enhance the power conversion efficiency of OPV devices by using systems of two or more donors and a fullerene acceptor, having complementary absorption spectra to cover a wider wavelength range of the solar radiation spectrum. Indeed, the photobehaviour of three blend systems with different combinations of five extended arylacetylenes and one arylvinylene, potentially interesting as active layers in OPV cells, evidenced a different behaviour in $CHCl_3$ solution from that in the thin-films. In $CHCl_3$ solutions the spectral and photophysical properties of the mixtures were the sum of those of the separated components. Conversely, the photobehaviour of the mixtures in the thin-films showed an efficient energy transfer among the singlet excited states of the mixture components that practically led to observe emission from the low-lying S1 state of the bathochromic species only. Its fluorescence was then efficiently quenched by PCBM. This interesting mechanism can be exploited in the construction of OPV devices, given that solar photons may be absorbed by an inefficient charge-donor (the hypsochromic mixtures components) thus extending the used zone of the solar spectrum. The collected photons can thus produce, by an efficient energy

transfer, the excited states of species with a higher capacity to give charge separation in the presence of the charge acceptor (PCBM).
Particularly noteworthy was the peculiar behaviour of the arylvinylene anthracene-derivative that showed a broad and weak fluorescence band in $CHCl_3$ and a sharp intense emission in thin-films (a case of aggregation-induced emission enhancement), making it particularly interesting for application.
Moreover, the spectral and photophysical behaviour of some arylacetylenes in solution was particularly investigated to study the influence of different substituents and cores in the structure.
Generally all these compounds showed a fluorescence deactivation as principal decay pathway in all the solvents. The cyclophane-anthracene-derivative, formed by two identical units connected by two butane-chains, generally showed a behaviour analogous to that of the single unit. The symmetric compound bearing two 2,1,3-benzothiadiazole groups showed the emission spectrum shifted toward the red with increasing the solvent polarity thus favouring the state stabilization of S_1 and internal conversion to S_0 as its principal deactivation pathway.
An unexpected and interesting behaviour was observed for the nitro-derivatives where a strong reduction of fluorescence was observed on passing from toluene to $CHCl_3$ while the intersystem crossing (ISC) to the triplet state remained practically unchanged. This behaviour was interpreted on the basis of the presence (evidenced by theoretical calculations) of an upper excited singlet state more polar than S_1. Even if little polar, $CHCl_3$, preferentially stabilizes the polar forbidden S_2 state with respect to the less polar S_1, thus reducing the S_1-S_2 energy gap, giving a strong increase of the S_1-S_0 internal conversion yield, analogously to what described in the Lim's proximity effect.
Furthermore, in order to understand the role of the intramolecular charge transfer (ICT) and ISC in the relaxation processes of the asymmetric derivatives, resort was made to emission and nano/femtosecond transient absorption measurements and to parallel quantum mechanical calculations at the TDDFT level. It was found that the excitation populates the lowest vibrational levels of the locally excited state which exhibits lifetimes strongly affected by the solvent and that the ICT process, which leads to the $^1CT^*$ state, becomes faster upon increasing the solvent polarity and takes place within few ps in highly polar solvents (with the exception of cyano-

and aldehyde-anthryl derivatives, owing to the absence of ICT states). In these solvents, the dramatic reduction of the fluorescence yield ϕF and the parallel decrease of the triplet yield ϕT indicate that an efficient internal conversion plays a fundamental role in the deactivation of the $^1CT^*$ state due to the preferential stabilization of the highly polar ICT* state in polar solvents and the consequent reduced $S_1–S_0$ energy gap.

When the central unit was the anthracene chromophore, a significantly red-shifted absorption spectrum was observed, making these compounds interesting in photovoltaics, whereas the fluorene central ring was found to favor transitions with high CT character, interesting for NLO applications. For the anthracene-derivatives, the high energy gap between S_1 and upper $^3(n,\pi^*)$ states, makes the spin–orbit coupling less efficient and the ISC slower than in the fluorene-derivatives. Both the ICT character of the lowest excited states and the ISC yields decrease in the order NO_2 > CHO > CN, in agreement with the electronic affinity and the energy of the $^3(n,\pi^*)$ state of the side groups.

Generally the investigated compounds showed a red-shifting only in the emission spectra with the increasing of solvent polarity (positive fluosolvatochromism), while the absorption spectra remained practically in the same wavelengths region. In this case it was possible to derive the first hyperpolarizability coefficient (β), that depends on the difference of the dipole moment between the excited singlet state and the ground state.

The obtained results showed that high values of β characterize the molecules with higher push-pull character, in particular in the case of the nitro-derivatives.

Lastly, two-photon induced fluorescence was registered with the apparatus assembled in our photochemistry laboratory during my PhD work, and the TPA cross section (δ) was calculated for some of the investigated compounds. The δ values were found to be larger than, or comparable to, that of a standard (e.g. fluoresceine), making these compounds interesting for NLO applications, such as photovoltaics, memory storage and microfabrication techniques.

It should be noted that the set-up for TP spectroscopy and the first (preliminary) results obtained are opening new ways and offering interesting possibilities in the study of NLO materials in our laboratory. In fact, this facility allows the direct measurement of an

informative NLO property such as the TPA δ, thus improving the actual research work, limited so far to derive the hyperpolarizability coefficient by the solvatochromic method.
In general, the results of this thesis work on a large series of compounds led to a comprehensive understanding of the structure characteristics suitable for different applications. The study of the effect of substituents in the symmetric/asymmetric compounds, the comparison between ethenyl and ethynyl π-bridges and the role of ICT processes provided interesting information which can be useful to adress the synthetic work towards oprimized materials having improved light harvesting, charge photogeneration efficiency and NLO properties.

EPA IS ON FACEBOOK

join EPA on Facebook ....

TECHNICAL NOTES

Detectors for Optical Spectroscopy Measurements.

All Modern spectroscopy measurement systems use a detector that can connect the incident light from a sample into an electrical signal. Correct selection of such a detector is critical to successfully measure, of course in previous articles the excitation, sample and wavelength selection devices before detector must be optimum for the application requirements. After all the famous USA baseball player, Walter Johnson (1887-1946) said "you can't hit, what you can't see" or to paraphrase "you can't measure what you can't detect" !

The output signal from the detector must be monitored, stored and analysed a spectroscopic measurement. As such, the signal-processing and readout system is extremely important to the overall performance of the system. The particular type of signal processing depends on the form of the output signal, the noise sources expected and the signal level itself. The signal-processing step can perform many conversions such as current-to-voltage, analog-to-digital conversion, amplification, or some mathematical operation designed to improve the measurement of signal-to-noise ratio. The key goals are to undertake the detection process in a stable, signal efficient manner with a high level of linearity with reflect to signal infinity as well as being repeatable. The final goal is to ensure a best detected signal-to-noise ratio.

The outputs of most detectors are used in the analogue mode. The exception to this the photomultiplier, which may be used in either analogue, current sampling, or in the photon-counting mode. Nearly all measurements are made by using an analogue-to-digital converter to convert the output of a detector to the digital domain for future processing, analysis and display. Even in digital measurements some conditioning, such as filtering or amplifying the analogue signal, is usually necessary to make it suitable for recording by the converter. In photon counting systems, the recorded signal is the number of pluses observed or counted. Photon counting is particularly useful in

applications where the signal irradiance is relatively low, such as fluorescence, Raman spectroscopy and some photoluminescence measurements. The two main categories of optical detectors are single channel and multi-channel. Single channel detectors have one detection element that records light at the exit slit of the monochromator. By scanning the monochromator, by rotating the grating, the detector can record one data point per grating position. In systems with, multi-channel detectors these may collect many wavelength points simultaneously without the need to scan the grating.

The choice of detector is very application dependent and is based upon several criteria, for example:

- the measurement principle to be used,
- the spectral range required,
- the amount of light available or sensitivity needed, as well as
- the expected time resolved or speed of measurement required.

As such these can be several specification or performances that are competing against each other as well as the need for detector and data acquisition is to fit within a specified budget constraint, while ensuring the measurement needs are met.

The main figures of merit for detectors are as follows:

- Quantum Efficiency
- Responsivity
- Noise-Equivalent Power (NEP)
- D*
- Capacitance
- Spectral Response, and
- Spatial Uniformity

Quantum Efficiency

$$QE = \eta = \frac{\text{No. photodetection events}}{\text{No. Incident photon}}$$

This is a wavelength dependent quantity in which a certain fraction of photon greater than the detector threshold energy.

Related to this is the spectral responsivity which is perhaps a better and more reliable figure-of-merit for detector comparison. It is also a wavelength dependent property and is related to detector QE. For all measurements the main goal is to maximise the signal-to-noise ratio and this is the key to success and is probably the single most important parameter. It therefore depends not only on the detector and its measurement mode, but also the ability of the system to get light from target efficiently and properly to the detector.

Signal-to-noise ration also leads directly yo the idea of Noise Equivalent Power (NEP) and the related D* figures of merit. This is a figure of merit most often quoted in relation to infra-red detecors and also sometimes quoted as a D* value that is the NEP essentially normalised to the detector area.

- NEP is the optical power required to give signal-to-noise of 1 (0dB) in a given bandwidth
- Expressed as: NEP (λ , f , BW)
- Very often normalised to detector area of $1cm^2$
  - and given in unit of $Wcm^{-1}\ Hz^{-1/2}$
- Detectivity = 1/NEP

The dominant noise process depends upon detector characteristics and the measurement mode that is being use be used. Reference to the data sheet of the detector is therefore important and an ability to review specifications under the same conditions is important to allow correct comparisons to be made.

It is important to match the detector response to the spectral requirements of the application. This should, hopefully, also help to ensure best signal-to-noise ratio. There is a very wide range of detectors, photo-diodes, photomultipliers, IR detectors based upon semiconductor (photon) as well as thermal properties. Each type has its unique spectral response curves and these may even change from batch to batch. Mostly, detector suppliers' present spectral response curves are given of a defined set of measurement conditions. For

example nearly all CCD QE curves are measured at room temperature 20 to 25°C, yet manufactures of CCD detector cameras specify noise at -80°C or lower temperatures. In many cases the QE at -80°C has dropped to perhaps half of the room temperature value. So for this reason its very difficult to really compare exact detector performances under read operating conditions. Typical QE values for photomultiplier and IR detector are demonstrated in figure 1 and 2.

.

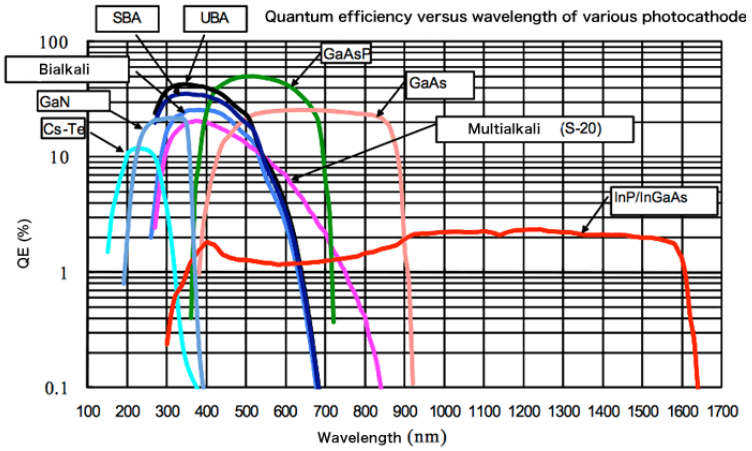

Figure 1: typical Quantum Efficiency curves for some detectors, courtesy of Hamamatsu Photonics

In the most basic form analogue detectors can be measured using analogue-to-digital connection (ADC). To use them effectively the signal is often pre- conditioned in terms of gain and offset. The available resolution of an ADC defines: -

- the number of discrete values it can produce over the range of analogue values.
- determines a lower bound on quantisation error.
- max possible average S/N ratio for ADC, and is

- Expressed in digital form as a number of bits.

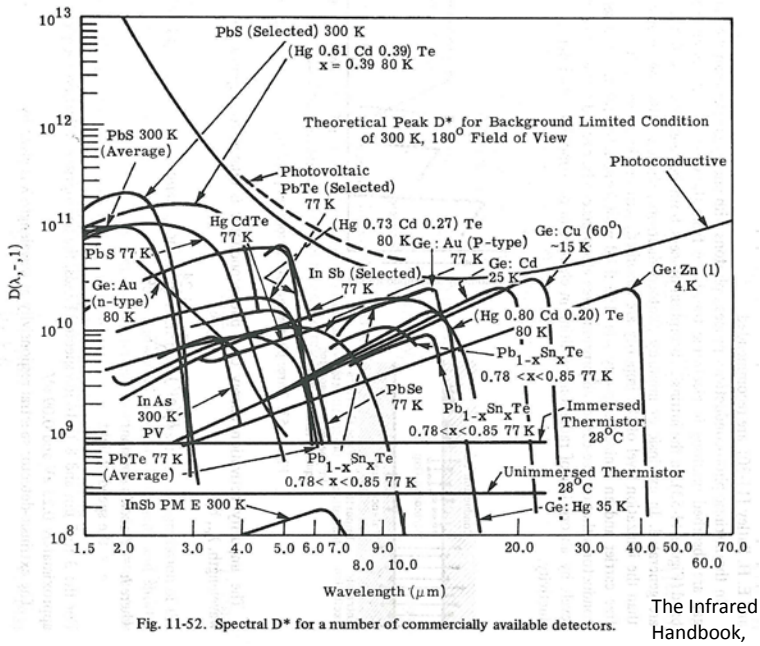

Figure 2: Infra-Red Detector Spectral Detectivity responses for IR detectors.

Resolution / bits	Steps	% change
8	225	0.392157%
10	1023	0.097752%
12	4095	0.024420%
14	16383	0.006104%
16	65535	0.001525%
24	16777215	0.000006%

Table 1: common ADC resolution and number of steps.

Since detectors can be used in either current (analogue) or photon counting (digital) modes how do we determine which measurement mode is optimum. The answer lies in the available light incident upon detector and the likely signal range (dynamic range needed). Hamamatsu Photonics has presented a rather nice summary graph and this is reproduced in figure 3 below.

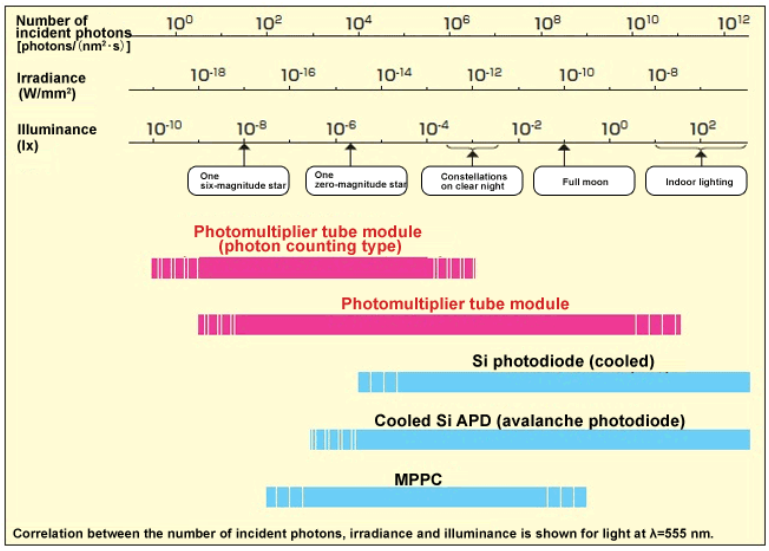

Figure 3: Detector and measurement choices in relation to light levels, courtesy of Hamamatsu Photonics.

In the infrared, the use of a mechanical chopper and a lock in-amplifier can be very effective. These allow the signal processing system to alternately measure the optical and dark noise signals and automatically subtract the dark noise. There can be significant advantages to the measured signal-to-noise ratio and signal stability by using such a technique. In fact, the use of such a synchronous demodulation system can literally recover signals that would otherwise be buried in the noise. Knowing at the same time 50% of the available optical signal is thrown away due to the chopping action.

The key action of a lock-in amplifier / chopper measurement is to set a measurement frequency and electrical band-pass that allows the out-of-band noise to be rejected, thus significantly improving signal-to-noise. The reduction in noise level of a useful signal at frequency, f_o, is proportioned to the square rout of the bandpass filler centred at that frequency.

If a signal is repetitive, particularly those from pulsed experiments, then a boxcar integrator can be an effective data acquisition tool. The box-car integrator allows the measurement of signals related to a trigger event and the rejection of all others.

Lock-in amplifiers and boxcar integrators provide analogue processing of the signal. Such methodologies can also be implemented in the digital domain using either hardware or software techniques. Photon-counting systems can be constructed where a digital lock-in approach is used. Thus, during the irradiated cycle the counter counts up and, during the dark cycle, counts down to remove the background signal.

- Analogue detectors and DC signal measurements are very useful for strong signals and in situations where interference is minimal.
- Lock-in amplifiers and choppers are very useful in measurements where the signal levels are weak or unstable due to other issues and in cases where the noise level could be comparable to signal level or higher. If in cases where the phase information is useful, such as timing or delay time measurements.
- Photon Counting is very useful in situations of low light detection and offers the possibility of the best sensitivity in many applications.

In Summary:

- Use DC measurement where you can.
- Use Photon Counting with photomultipliers or single photon counting photo-diodes with weak signals.

- Use Lock-in Amplifiers and Choppers for weak signals with strong noise levels or interference.
- Check and double check that the signal you measure is a real optical signal.

Dr. John R. Gilchrist
Gilden Photonics Ltd

References

1. The Infrared Handbook, WL Wolfe & GJ Zissis, Office of Naval Research 1978
2. SpectroChemical Analysis, JD Ingle jr & SR Crouch, Prentice Hall 1988
3. The Art of Electronics, P Horowitz ansd W Hill, Cambridge University Press, 1981
4. Photomultiplier Tubes: Basics and Applications , Hamamatsu Photonics. 1999
5. PhotoMultiplier Tubes: Principles and Applications, Photonis, 2002
6. Building Electro-optical Systems 2nd Ed, PCD Hobbs, Wiley, 2009
7. Noise and fluctuations in electronic devices and circuits, FNH Robinson, Clerndon Press, 1974
8. Charge Transfer Devices in Spectroscopy, Eds: JV Sweedler, KL Ratzlaff, M Bonner Denton, VCH Publications , 1994
9. Fundamentals of Scientific Charge-coupled Devices: v. PM83 (SPIE), J R Janesick, SPIE Society of Photo-Optical Instrumentation Engineers, 2001

PHOTOCHEMICAL AND PHOTOBIOLOGICAL SCIENCES

CONFERENCE REPORTS

Italian Photochemistry Meeting 2013

From November 28th to Dicember 1st the annual meeting of Gruppo Italiano di Fotochimica (GIF) was held. The venue was a Hotel (Figure 1) in a location at the edge of the ski area of the Province of Potenza. Rifreddo is a locality situated 1146 meters above sea level, and the Jubilee Hotel is on the edge of the great forest of Rifreddo.

Figure 1. Hotel Giubileo di Rifreddo (PZ)

. The meeting has been organized by the photochemical group of the University of Basilicata to which the writer belongs but also Prof. Rocco Racioppi, and doctors Licia Viggiani, Sonia Stoia, Ambra Guarnaccio, and Federico Rofrano. The conference was attended by over sixty researchers from many areas of Italy (Figure 2). The participants were composed largely of very motivated young researchers in the field. This was wanted in relation to a long tradition of national conferences of photochemistry, whose goal is to provide a forum where in particular young people can present their work and compare their work with that of their colleagues.

Figure 2. Participants to the meeting.

The conference was held over two full days of conference activities. Four plenary lectures and twenty-two oral communications were presented The program was completed by a poster session where fourteen communications were presented and which has occupied the entire afternoon of the second day of the conference.
The first plenary lecture of the conference was given by James Lanzani of the Politecnico di Milano, member of the Italiana Institute of Technology of Genoa. The report (Interface dynamics in organic photovoltaics) has demonstrated the potential application of

the time-resolved transient spectroscopy to characterize the physical and chemical phenomena that occur in new semiconductor materials used in the design of new photovoltaic collectors. There has shown how the use of pump and probe spectroscopy resolved to femtoseconds allows to understand that a polymer potentially useful as photovoltaic collector characterized by a low value of the band gap dissipates the excess energy by an internal conversion process.

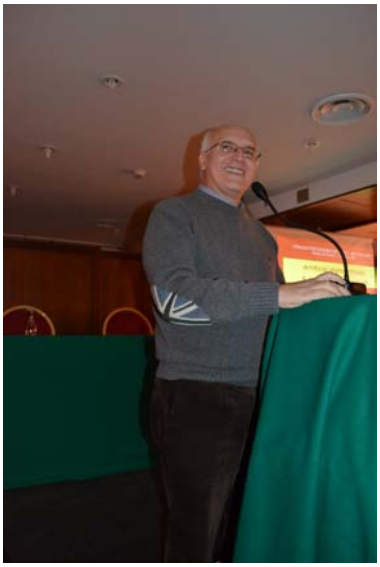

Figure 3. Sebastiano Campagna during his talk.

However, if in the system an electron acceptor is present then the charge separation process becomes fast enough to compete with the internal conversion . Sebastiano Campagna, University of Messina, held the second plenary lecture of the first day of the conference (Figure 3). His report (Artificial photosynthesis: a supramolecular approach) has focused on supramolecular models developed in his group that allows an approach to artificial photosynthesis. The problem is very important and not easy to solve, because it requires the use of biomimetic systems structurally organized in such a way as to interact and perform functions closely integrated with each other. Different approaches have been proposed based on the design of

antenna systems able to act as collectors of sunlight and to convert it into electronic energy, systems capable of using the collected energy to achieve charge separation processes, and systems able to catalyze multielectronic transfer processes.

The second day saw the plenary lecture of Gianluca Farinola and John Gilchrist. Gianluca Farinola (University of Bari) discussed two cases in which photoactive substances have been combined in natural systems allowing the formation of nanostructured hybrid. In one case, the type aryleneethynylene dyes were combined with the photosynthetic system of *Rhodobacter sphaeroides* bacterium by increasing the photosynthetic capacity of the system. In the second case, the same type of dyes was joined to diatoms. John Gilchrist (Gilden Photonics Ltd.) has discussed the problems associated with the development of new instruments (spectrophotometers for example) in the field of photochemical pollution. In particular focused on the design of a spectrofluorimeter Whereas the problems connected to the fact that the observed spectrum is the convolution of the experimental system and the true emission spectrum.

Fig. 4. Prize giving of oral commincations: from left Elena Selli, president of the GIF and Interdivisional Photochemistry Group of SCI, Ambra Guarnaccio, Grazia Chiara, Enrico Marchi and Maurizio D'Auria, for the Organizing Committee**.**

The Gilden Photonics has generated a prize for the best oral presentation. The committee discussed at length by examining the potential candidates and decided to consider three oral presentations: that of Chiara Grazia, University of Perugia, Enrico Marchi, University of Bologna, and Ambra Guarnaccio, of the University of Basilicata (Figure 4). Having to deliver the prize, this was attributed to the dr. Enrico Marchi.

To conclude this brief presentation, we, as organizers of the conference, we hope that it has provided a useful opportunity to reflect on the potentialities of a discipline that has to deal with a sustainable development of our society and we hope we realized this goal.

Maurizio D'Auria

MEMBERSHIP APPLICATION FORM

EUROPEAN PHOTOCHEMISTRY ASSOCIATION
2011 MEMBERSHIP RENEWAL/APPLICATION FORM

Please complete the form and send it to the Treasurer by mail or fax
(do not use e-mail for security reasons!):
Dr. Silvio Canonica Eawag, W+T Dept.
Ueberlandstrasse 133, P.O. Box 611, CH-8600 Dübendorf, Switzerland
(Fax +41 44 823 5210)

I wish to renew/apply for membership of the European Photochemistry Association (EPA)

Family name: **First name:** **Middle initial(s):**

Date of birth (dd/mm/yyyy)**:**

If you are applying for a new membership or if your contact details have changed, please fill in the following section:

Address: (Please use your institutional address)

Tel: **Fax:** **Email:**

Membership fees for 2011 in EUR **(please check one box)**

The membership fee includes electronic subscription to the EPA official journal *Photochemical & Photobiological Sciences*, the EPA Newsletter and reduced conference fees.

regular	☐ **30** EUR
student*	☐ **15** EUR * please supply attestation

For countries with economic difficulties, a reduced fee of 15 EUR can exceptionally be applied on request (only upon written approval by the Treasurer).

Alternative methods of Payment **(please fill in either 1. or 2.)**

1. **Credit card**. Please fill in the details below (all details compulsory).
I, the undersigned, authorise the European Photochemistry Association to debit my credit card:
☐ MasterCard ☐ Visa
Card number Expiry date: For the sum of EUR
Amount of EUR in words:
Name of card holder: Signature of card holder:
Security code: _ _ _ (this code corresponds to the last three digits to the right on the back of your credit card)

2. **Bank order** to UBS AG, Roemerhofplatz 5, P.O. Box 38, CH-8030 Zürich, BIC (Swift): UBSWCHZH80A
Account holder: European Photochemistry Association, c/o Dr. Silvio Canonica, 8600 Dübendorf
IBAN: CH27 0025 1251 8404 5260 C
I herewith certify that I effected a bank transfer on (fill in date) for the sum of EUR
to cover the EPA membership fee for the year(s) 2011 - . Signature of the member:
Please ensure that you are clearly identified on the bank order.